5-2020

Using Infrared Radiometry Thermometer for Irrigation Management of Dry Edible Beans in Western Nebraska

Isabella Presotto Possignolo
University of Nebraska - Lincoln, ipresottopossigno2@huskers.unl.edu

USING INFRARED RADIOMETRY THERMOMETER FOR IRRIGATION MANAGEMENT OF DRY EDIBLE BEANS IN WESTERN NEBRASKA

by

Isabella Presotto Possignolo

A THESIS

Presented to the Faculty of

The Graduate College at the University of Nebraska

In Partial Fulfillment of Requirements

For the Degree of Master of Science

Major: Mechanized Systems Management

Under the Supervision of Professor Xin Qiao

Lincoln, Nebraska

May, 2020

USING INFRARED RADIOMETRY THERMOMETER FOR IRRIGATION MANAGEMENT OF DRY EDIBLE BEANS IN WESTERN NEBRASKA

Isabella Presotto Possignolo, M.S.

University of Nebraska, 2020

Advisor: Xin Qiao

United States is the leading producing country in the world for dry edible beans (DEB) and one of the most important states for DEB production is Nebraska. About 74% of DEB production in the state is in western Nebraska and more than 90% are produced under irrigated land. However, farmers in the region are challenged by unstable availability of surface water and limited ground water resources. Therefore, water-saving and yield-preserving irrigation management practices are crucial to secure and sustain DEB production in western Nebraska. In Chapter One, we compared different irrigation management strategies including deficit and limited irrigation on the effect of saving water with minimum penalty on yield for DEB. However, due to experimental error in 2018 and severe hailstorm in 2019, we were not able to appropriately evaluate the performance of the irrigation management practices.

Proper irrigation management requires farmers to determine the right timing and amount to irrigate. Soil water sensors are the most popular sensor-based approach used by farmers to decide when and how much to irrigate. However, installation or retrieval of soil water sensors require excavation of soil and can be challenging. Other than soil water sensors, there are plant-based water stress monitoring technology that are less soil

disturbing such as infrared radiometry thermometer (IRT). Using canopy temperature measured from IRT, researchers can calculate thermal-based indices such as crop water stress index (CWSI) for many crops around the world. Yet limited research focus on detecting water stress of DEB using IRT and CWSI. Therefore, in Chapter Two, we quantified parameters (baselines) that are crucial to calculation of CWSI using canopy temperature measured from IRT; and evaluated the performance of calculated CWSI under four irrigation treatments that ranged from dryland to fully irrigated for DEB in Nebraska. The average lower baseline of DEB found was $T_c - T_a = 2.78 - 1.59$ VPD ($n = 25$, $R^2 = 0.81$) and upper baseline was $T_c - T_a = 3.76$ ($n = 11$, SD = 0.42). Afternoon CWSI (12:00 PM to 3:00 PM) showed significant difference among the irrigation treatments, with p-values of 0.0143 (2018) and 4.2×10^{-6} (2019).

ACKNOWLEGEMENTS

First of all, I would like to thank God for providing this opportunity and for all the blessings during my studies and research at University of Nebraska Lincoln/Panhandle Research and Extension Center.

Second, I would like to thank my family for always being by my side and supporting me, my boyfriend Vinicius Perin for helping me through this journey, and all my friends for the assistance during those years of study/research.

Third, I would like to thank Dr. Xin Qiao for all the teaching and patience, Dr. Derek Heeren, for all the support and all the committee members Dr. Suat Irmak, Dr. Daran Rudnick and Dr. Kendall DeJonge for all the assistance. Also, I would like to thank Mr. Les Kampbell, Dr. Liang and all the interns who helped me in this research.

TABLE OF CONTENTS

LIST OF TABLES

Table Page

LIST OF FIGURES

Figure Page

CHAPTER 1. DEFICIT AND LIMITED IRRIGATION MANAGEMENT FOR DRY EDIBLE BEANS

Abstract

Irrigation plays an important role in the dry edible bean (DEB) production, especially in the western Nebraska. The region is considered a semi-arid region and more than 90% of its DEB production is under irrigated land. Since water resources are limited in this region, it is imperative to adopt sustainable irrigation management techniques to increase irrigation water efficiency (IWUE) for successful DEB production.

To address this issue, previous researchers implemented deficit irrigation (DI) and limited irrigation (LI) aiming to increase IWUE. These methods focus on applying less water than the total plant water requirement and still assure competitive crop yields. The main challenge of using these methods is finding the right time or amount to apply to prevent significant reduction in crop yields. The main objective of this chapter was to find the best scenario of DI and LI for DEB in western Nebraska, that would have the highest water conservation with the least impact on yields.

In 2018, IWUE ranged from 0.01 to 0.34 Kg m^{-3}, with average of 0.11 ± 0.10 Kg m^{-3} and yields ranged from 3.12 to 3.35 Mg ha^{-1} with average of 3.24 ± 0.08 Mg ha^{-1}. Unfortunately, in 2019, yields were sharply reduced and IWUE was not calculated due to multiple hailstorms. Due to extreme weather conditions in both years (heavy rainfall in 2018 and hailstorms in 2019), the optimum DI and LI strategies were not found.

1.1. Introduction

Dry edible bean (*Phaseolus vulgaris L.*) is an important source of protein and fiber and has a critical role in human nutrition. The U.S. is the sixth-leading world producer of dry edible beans (DEB) and produced 37.4 million cwt (hundredweight) in 2018 (USDA, 2019). Among DEB producing states, Nebraska is the leader with about 74% of its production located in western Nebraska. Area of DEB production in Nebraska ranges from 56,000 to 80,000 hectares (https://cropwatch.unl.edu/drybeans) and more than 90% of DEB in the area is under irrigation. Reason for dominating production acreage under irrigation is due to the semi-arid climate in western NE where crop evapotranspiration (ET_c) of DEB usually surpass rainfall amounts during the growing season (June to September).

In western Nebraska, freshwater resources for irrigation comes from two main sources– surface and groundwater. Surface water is mostly from snowpack melt of the Rocky Mountains in Colorado and Wyoming (Yonts et al., 2018), and availability is highly unstable due to dependence on the variable snow events received each year (Dettinger, 2005). On the other hand, groundwater originates mainly from the High Plains (Ogallala) aquifer or other secondary aquifers (e.g. Chadron Aquifer and Upper Cretaceous aquifer) (Divine and Sibray, 2017), and irrigated lands that use groundwater are subject to mandatory allocation. Irrigators can be restricted to use 60-70 inches in a five-year period (https://www.npnrd.org/water-management/integrated-management-plan.html). Long-term agricultural water use has also caused serious depletion of groundwater aquifers (Tracy et al. 2019) with low annual recharge rates. The Ogallala aquifer in western Nebraska, for example, presents a recharge rate between 2 and 5 mm

per year (Scanlon et al., 2012). Under this scenario, it is imperative to implement irrigation management practices that use water more efficiently.

Deficit irrigation (DI) and/or limited irrigation (LI) have been studied by researchers to improve irrigation water use efficiency while maintaining yield. To avoid significant yield losses in regions where water is limited, researchers have been studying the application of DI and LI (Calvache et al., 1997; Bourgault et al., 2013; Yonts et al., 2018). DI refers to applying less water than plant water requirement during certain growth stages (i.e. vegetative and reproductive) that are less sensitive to water stress; and LI refers to distribution of the seasonal total available water in less than optimal equal amounts along the season, not accounting for crop growth stages (Irmak and Rudnick, 2014).

Several studies showed that employing DI and LI in agriculture can be economically beneficial for farmers who are located in semi-arid regions (English, 1990; Fereres and Soriano, 2006; Geerts and Raes, 2009; Mahmoudzadeh Varzi et al., 2019). Even though yields may not be as high as yields achieved with full irrigation, crops under DI and LI can have competitive yields if DI and LI strategies are carefully chosen. In a study with wheat in Turkey, it was shown that if DI is applied to wheat's milk stages, a 35% deficit of total plant water requirement will only lead to a 2% in yield reduction, and a 65% deficit of total plant water requirement irrigation will lead to a 7% yield reduction (Tari, 2016).

Variation in season rainfall can affect yields when using DI/LI strategies. For maize under a limited irrigation scenario in southeast Nebraska, Irmak (2014) found that in three out of five years of the study period, a 25% deficit leads to less than 5% yield

losses and in wet years, a 40% deficit could lead to ~6% yield loss. In western Nebraska, similar results were observed by Yonts et al. (2018) on DEB. The authors found that irrigation treatments with 25% deficit of full irrigation along the entire season of DEB can result in less than 3% yield reduction. The authors also mention that in wet years, irrigation treatments with 50% deficit in the vegetative and pod filling stages caused less than 5% yield reduction.

A key term when evaluating DI and LI strategies is the irrigation water use efficiency (IWUE), which is defined as the relationship between crop yield and the total depth of water applied for irrigation. This concept was first introduced by Bos (1980) as the water supply ratio. The formula used to calculate IWUE is represented below (Irmak et al., 2011):

$$\text{IWUE} = \frac{(Y_i - Y_d)}{IR}\ x\ 100 \quad (1)$$

Where IWUE is irrigation water use efficiency in (Kg m^{-3}), Y_i is irrigated crop yield (Mg ha^{-1}) in megagrams per hectare, Y_d is dryland crop yield (Mg ha^{-1}), and *IR* is the amount of irrigation water applied (mm).

Previous studies have shown that DI and LI can increase IWUE (Tari, 2016; Yonts et al., 2018; Al-Ghobari and Dewidar, 2018). Yonts et al. (2018) reported that for DEB in western Nebraska, IWUE increased in average by 26% when reducing irrigation amount by 25%. In some cases, higher IWUE can be observed for lower irrigation treatments. Kuşçu et al. (2014) reported that an increase of 42% in IWUE was observed

with water savings of 33%. The authors also mentioned that water stress should be scheduled at certain stages to have minimal impact on yields.

The DI timing is a crucial factor when aiming to reduce yield losses. Payero et al. (2009) mentioned that maize yield could have a variation of up to 33% depending on irrigation timing and the amount applied. Comas et al. (2019) found that for maize, implementation of deficit irrigation should take place in the late vegetative stages (V8-VT), instead of during grain filling stages (R4-R6), to minimize yield losses. Usually, the same crop will have similar sensitivity to drought growth stages. However, divergent results can also be found for timing of DI applications. For DEB, Calvache et al. (1997) report that the flowering stage was the most sensitive stage to water stress, while Simsek et al. (2011) report that the vegetative stage was the most sensitive to water stress, which could possibly be due to the different varieties used in the studies (cv. Imbabello and cv. Gina, respectively). Therefore, when implementing DI and LI strategies, it is important to bear in mind that using information from existing literature might not lead to similar results than the one found by previous research.

In order to determine the best timing of when to apply DI, researchers stress the plants at different growth stages, generally dividing into two stages (vegetative and reproductive). However, different strategies may be applied. Yonts et al. (2018) conducted a study in western Nebraska and divided the DEB growth stages in three groups: vegetative, flowering and pod filling, having three different irrigation amounts for the different growth stages. Another approach is setting specific monthly irrigation amounts during the crop growing season. Payero et al. (2009), in a study of maize in

North Platte, NE, USA, used the three months of the growing season (July, August and September), to set the different irrigation treatments.

The main challenge of using DI and LI practices is finding the right timing of deficit irrigation application and the lowest threshold of irrigation depth that will not lead to substantial yield losses. Each crop responds differently to water stress, and the response varies depending on water deficit timing, intensity, and duration (Geerts and Raes, 2009). Therefore, the objective of this study is to determine and evaluate DEB yield response considering different DI and LI scenarios.

1.2. Materials and Methods

1.2.1. Study location

The experiment was conducted under a variable rate irrigation (VRI) linear sprinkler (Zimmatic, Lindsay Corporation, Omaha, NE, USA) at the University of Nebraska Lincoln Panhandle Research and Extension Center (PHREC; 41°53'34.93"N, 103°41'2.04"W, elevation: 1189 m) in Scottsbluff, NE. The 4-span VRI covers 6.5 hectares of land. Soil under the VRI is a Tripp very fine sandy loam with bulk density of 1.32 (Mg m^{-3}) and the field has slopes of up to 3% in the north/south direction. Soil water holding capacity is between 15 and 17 %, with field capacity between 25 - 27% and permanent wilting point between 10 - 12%. The climate in the region is semi-arid, with a long term average (1982 – 2016) accumulative annual precipitation of 297 mm. The groundwater table depth at the site is around 14 m, the average (1982 – 2016) relative humidity is 60% and average high and low temperatures are 17° C and 1° C (Yonts et al., 2018). No nitrogen fertilizer was added to the study area.

1.2.2. Experimental design

Great Northern beans (variety Draco) were planted at 55 centimeters row spacing in 2018 and 2019. Planting dates, harvest dates and plot design for the two field seasons are summarized in Table 1.1. In 2018, the experiment design was a randomized complete design (RCD), while in 2019 it was a randomized complete block design (RCBD); treatments were divided into three different blocks (North – Block1, Middle – Block 2, and South – Block 3). Change of experiment plot design was to account for slope variability in the field in north-south direction. Even though slopes are mild in the field (up to 3%), southern plots still flooded during heavy rainfall events. Figure 1.1 shows the southern plots after a 44 mm rainfall that lasted approximately one hour on July 16th, 2018. A pump was used in the area for two days to drain the water.

Table 1.1. Planting dates, harvest dates and plot design for growing season during 2018 and 2019.

	2018	2019
Planting Date	June 7th	June 11th
Harvest Date	October 19th	October 4th
Plot dimensions	10 m wide x 15 m long	13 m wide x 15 m long
Number of rows per plot	18 rows	24 rows

Figure 1.1. South plots flooded after heavy rainfall (44 mm) in 2018.

1.2.3. Irrigation Treatments

There were 12 irrigation treatments in 2018 and 8 irrigation treatments in 2019, which varied from rainfed to over irrigation. Irrigation treatments were indicated as percentage of full irrigation, which were determined to fully satisfy plant water need. A description of each treatment, which was divided into three different stages, can be seen in Table 1.2. Plot design can be found in Figure 1.2 and Figure 1.3. Both DI and LI treatments were chosen for this experiment based on previous research (Simsek et al., 2011; Yonts et al., 2018). Yonts et al. (2018) identified three water-using stages for DEB: vegetative, flowering and pod filling. By stressing crop with different percentages of total plant water need in those three stages, one could determine which DEB growth stage is more susceptible to irrigation limitation/restriction. In addition, by dividing in three stages, it is possible to simulate real situations during the growing seasons for famers who get water cutoff periods by the irrigation districts.

Table 1.2. Treatment numbers and description of irrigation treatments applied in 2018 and 2019. Irrigation description represents percentage of full irrigation applied during vegetative, flowering and pod filling stages.

Treatments	Vegetative-Flowering-Pod Filling (2018)	Vegetative-Flowering-Pod Filling (2019)
1	0%-0%-0%	0%-0%-0%
2	33%-33%-33%	33%-33%-33%
3	66%-66%-66%	66%-66%-66%
4	100%-100%-100%	100%-100%-100%
5	133%-133%-133%	133%-133%-133%
6	75%-75%-75%	50%-100%-50%
7	50%-100%-50%	25%-75%-50%
8	25%-75%-50%	100%-0%-0%
9	0%-100%-33%	-
10	0%-100%-0%	-
11	100%-75%-50%	-
12	100%-50%-50%	-

The full irrigation treatment (FIT, 100%-100%-100%, Treatment 4) was meant to fully satisfy crop water needs by supplementing crop water consumption at bi-weekly basis. At each irrigation event, rate of FIT was calculated based on accumulated ET_c calculated using the single crop coefficient (K_c) method presented in FAO-56 (Allen et al., 1998). Daily reference crop evapotranspiration (ET_o) was retrieved from a station of Automated Weather Data Network (AWDN, http://awdn.unl.edu/classic/home.cgi, located about 0.25 km from experiment field) (Figure 1.4). The AWDN weather station was also used to collect hourly air temperature, relative humidity, solar radiation, wind speed and precipitation.

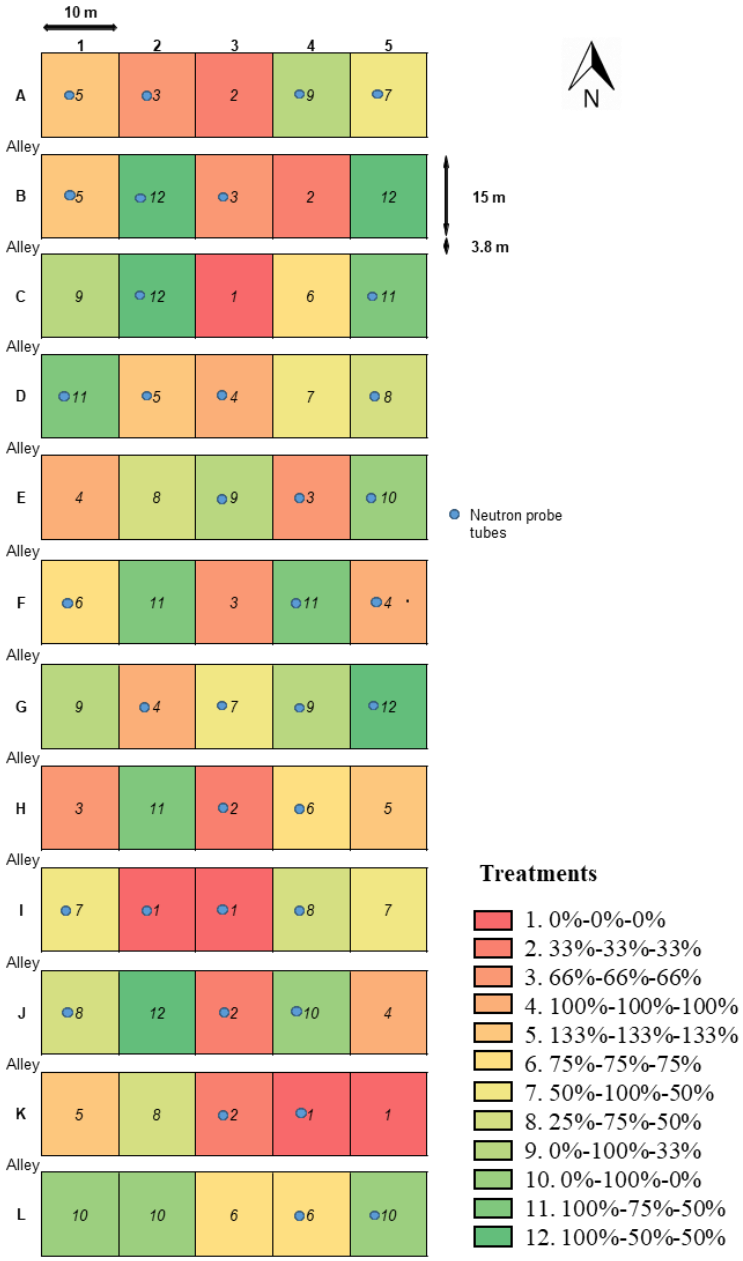

Figure 1.2. Plot maps for 2018. Numbers and colors represent different irrigation treatments. Blue circles represent locations where neutron probe tubes were placed. Treatments are represented in percentage of total crop water need. Irrigation treatments are: 1 (0%-0%-0%), 2 (33%-33%-33%), 3 (66%-66%-66%), 4 (100%-100%-100%), 5 (133%-133%-133%), 6 (75%-75%-75%), 7 (50%-100%-50%), 8 (25%-75%-50%), 9 (0%-100%-33%), 10 (0%-100%-0%), 11 (100%-75%-50%), and 12 (100%-50%-50%).

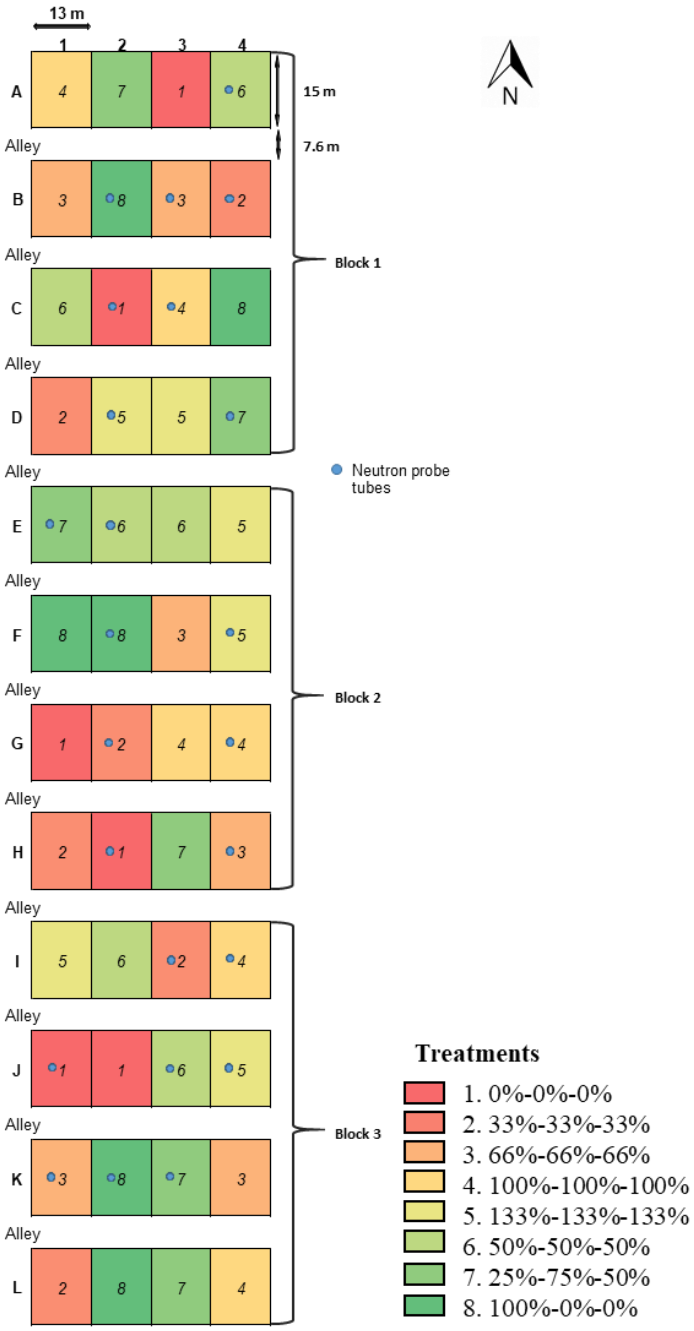

Figure 1.3. Plot maps for 2019. Numbers and colors represent different irrigation treatments. Blue circles represent locations where neutron probe tubes were placed. Treatments are represented in percentage of total crop water need. Irrigation treatments are: 1 (0%-0%-0%), 2 (33%-33%-33%), 3 (66%-66%-66%), 4 (100%-100%-100%), 5 (133%-133%-133%), 6 (50%-50%-50%), 7 (25%-75%-50%), and 8 (100%-0%-0%).

Figure 1.4. Weather station from Automated Weather Data Network (AWDN) used to collect meteorological data for this experiment.

Crop coefficient (K_c) was adopted from the table of Crop Water Use by Growth Stage – Dry Beans (Figure 1.5) provided by the Nebraska Agricultural Water Management Network (NAWMN) (http://nawmn.unl.edu). Details of NAWMN can be found in Irmak et al. (2010). Table presents weekly ET_{gage} values, which is used to monitor ET_o. However, for this study, only data for crop coefficient (K_c) (second column) was used, which was linearly interpolated between growth stages when crop presented certain canopy cover percentage described in the first column of table (Figure 1.5). Therefore, if the crop presented a 50% canopy cover, the K_c would be 0.48, and that value would be linearly interpolated until reaching 80% canopy cover ($K_c = 0.81$).

Crop Water Use by Growth Stage – Dry Beans

University of Nebraska Lincoln EXTENSION

Weekly ETgage® Change in Inches

Crop Stage	Kc	1.00	1.10	1.20	1.30	1.40	1.50	1.60	1.70	1.80	1.90	2.00	2.10	2.20	2.30	2.40	2.50	2.60	2.70	2.80	2.90	3.00
Emergence - 10%	0.06	0.06	0.07	0.07	0.08	0.08	0.09	0.10	0.10	0.11	0.11	0.12	0.13	0.13	0.14	0.14	0.15	0.16	0.16	0.17	0.17	0.18
Cover 10 - 50%	0.06	0.06	0.07	0.07	0.08	0.08	0.09	0.10	0.10	0.11	0.11	0.12	0.13	0.13	0.14	0.14	0.15	0.16	0.16	0.17	0.17	0.18
Cover 50 - 80%	0.48	0.48	0.53	0.58	0.62	0.67	0.72	0.77	0.82	0.86	0.91	0.96	1.01	1.06	1.10	1.15	1.20	1.25	1.30	1.34	1.39	1.44
Cover 80% - Full	0.81	0.81	0.89	0.97	1.05	1.13	1.22	1.30	1.38	1.46	1.54	1.62	1.70	1.78	1.86	1.94	2.03	2.11	2.19	2.27	2.35	2.43
Full Cover	1.00	1.00	1.10	1.20	1.30	1.40	1.50	1.60	1.70	1.80	1.90	2.00	2.10	2.20	2.30	2.40	2.50	2.60	2.70	2.80	2.90	3.00
Pod Elongation	1.00	1.00	1.10	1.20	1.30	1.40	1.50	1.60	1.70	1.80	1.90	2.00	2.10	2.20	2.30	2.40	2.50	2.60	2.70	2.80	2.90	3.00
Pod Fill	0.83	0.83	0.91	1.00	1.08	1.16	1.25	1.33	1.41	1.49	1.58	1.66	1.74	1.83	1.91	1.99	2.08	2.16	2.24	2.32	2.41	2.49
Dry Down	0.59	0.59	0.65	0.71	0.77	0.83	0.89	0.94	1.00	1.06	1.12	1.18	1.24	1.30	1.36	1.42	1.48	1.53	1.59	1.65	1.71	1.77
Senescence	0.30	0.30	0.33	0.36	0.39	0.42	0.45	0.48	0.51	0.54	0.57	0.60	0.63	0.66	0.69	0.72	0.75	0.78	0.81	0.84	0.87	0.90
Maturity	0.09	0.09	0.10	0.11	0.12	0.13	0.14	0.14	0.15	0.16	0.17	0.18	0.19	0.20	0.21	0.22	0.23	0.23	0.24	0.25	0.26	0.27

This chart can be used with readings from an ETgage® or other ET reference. First, identify the change in the ET rate across the horizontal row and then identify the current growth stage in the left column. Follow the two columns to the point where they intersect to identify the ET rate to use in your irrigation scheduling. When planning irrigation, account for soil moisture, precipitation, weather conditions, and the ET rate for growth stage of your crop.

Figure 1.5. Crop water use by growth stage for dry edible beans provided by Nebraska Agricultural Water Management Network (NAWMN). K_c values along the season were determined by interpolating the value from one row to the next according to the canopy cover percentage change along the season.

Canopy cover and growth stages of DEB were recorded on weekly basis. Canopy cover was calculated using an in-house programmed Crop Canopy Image Analyzer (CCIA), using pictures taken from plots at regular temporal interval (Figure 1.6). CCIA utilizes Mahalanobis distance and Canny edge detection method to estimate canopy cover and leaf shape factor, respectively. More details of CCIA can be found in Liang et al. (2019). During 2018, images were taken on July 6th, July 27th, and August 9th. During 2019, images were taken on July 18th, July 22nd, August 1st, and August 14th.

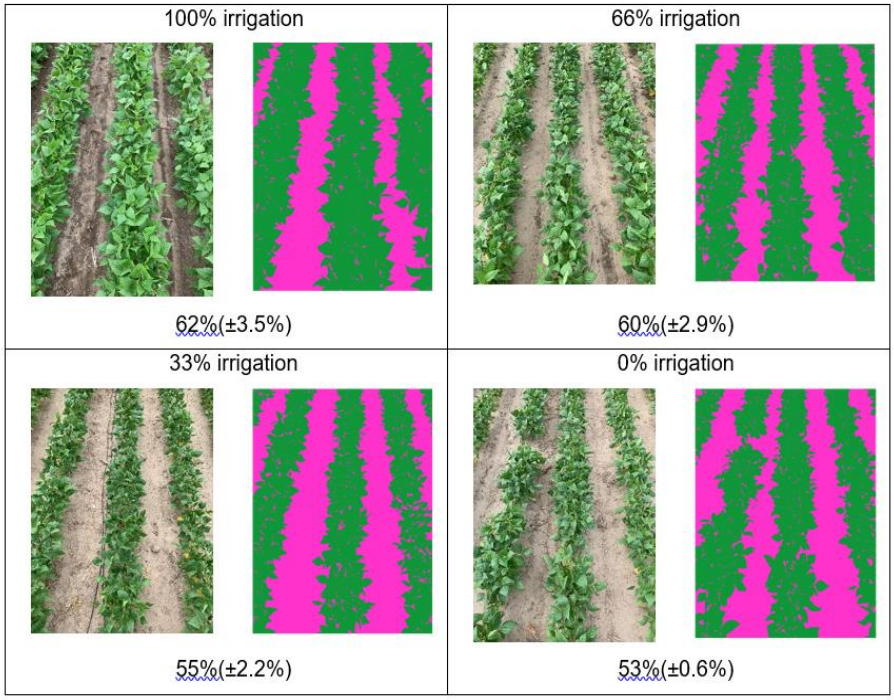

Figure 1.6. Example of canopy cover calculation using Crop Canopy Image Analyzer (CCIA) for pictures taken on 07/22/19, during the V7/V8 dry edible bean growth stage. Percentage values (62%, 60%, 55% and 53%) represent canopy cover percentage and values with ± inside the parenthesis (3.5%, 2.9%, 2.2% and 0.6%) represent the variation in canopy cover among the three images taken from different plots from the same treatment.

Three pictures from different plots with the same treatment were taken and analyzed separately. Average from the three analysis was then calculated for each

treatment. Pictures were taken at DEB canopies nearby IRT of each irrigation treatment with a RGB camera (1500×1125 pixels) on a tablet (Samsung Galaxy Tablet 10, Samsung Group, Seoul, South Korea) at a distance of approximately 30 cm height above the canopy at 45 downward degrees.

1.2.4. Procedures to implement Variable Rate Irrigation (VRI) for different irrigation treatments

The experimental field under the VRI follows typical crop rotation in western NE, which is: Corn – Dry Bean – Sugar Beet. Each span is planted with one crop and rotates to another crop in the following year. Spans are numbered from one to four from west to east. Span number two and span number three were used for this experiment in 2018 and 2019, respectively. Each drop on the VRI is connected to a solenoid valve that can be controlled individually. Each four adjacent solenoid valves are grouped into one bank and are controlled by a wireless node (Figure 1.7) that communicates to the central VRI computer. A GPS on the west end of the sprinkler detects position of the drop/nozzle and pulses the solenoid on and off to apply right amount of irrigation.

To provide accurate irrigation rates for all treatment plots, a GPS-referenced plot map was drawn and imported into FieldMAP (Lindsay Corporation, Omaha, NE, USA) to create prescription map. Then the prescription maps were loaded to control computer located at cart of the linear VRI on the west side. Details on how plot map was created, and how irrigation prescription map was uploaded into the linear irrigation system can be found in Appendix A.

Figure 1.7. Solenoids, drops, and nozzles of variable rate irrigation (VRI) system and wireless control nodes (white boxes pointed by yellow arrows).

1.2.5. Soil water monitoring

Soil water content was measured weekly by using a neutron probe (CPN 503 DR Hydroprobe, Concord, CA, USA). Aluminum access tubes were installed, and neutron probe was lowered into the tube to measure soil water content. In 2018, 36 tubes (12 treatments x 3 repetitions) were installed and in 2019, 24 tubes (8 treatments x 3 repetitions) were installed at the plots to a 1.4 m depth. Tubes were placed in the middle of the plots in the crop row (crop row number 9 in 2018 and number 12 in 2019). Standard count readings were taken before and after taking actual readings. Then 30-second readings were taken at four different depths: 30, 60, 90 and 120 cm. A previously developed calibration equation (Equation: STD x 2.3622 – 0.3629, R^2 = 0.96 and n = 19) was used to transform neutron probe readings into soil volumetric water content (VWC):

$$VWC\ (\%) = \frac{(\mathrm{NP}) \times 0.93}{STD\ \times 2.3622 - 0.3629} \times \frac{1}{12} \times 100 \qquad (2)$$

where NP is the neutron probe reading, STD is the average standard count and 0.93 is the calibration coefficient (Formula is multiplied by 1/12 to eliminate the units since data was presented in inches per feet and by 100 to obtain the value in percentage).

Also, water content was calculated for the top 60 cm of water by multiplying the 30 and 60 cm VWC (decimal) by 12 inches. The two values were summed up and multiplied by 25.4 to transform into mm of water.

1.2.6. Dry edible bean yield data processing and analysis

Dry edible beans were harvested using a 9500 John Deere combine equipped with a GPS reference yield monitor (AgLeader Technologies, Ames, Iowa, USA). Yield maps were imported into ArcGIS Pro (Esri, Redlands, California, USA) to calculate mean and standard deviation of yield within each plot. Yield values in alleys were discarded. Treatment yields were analyzed by employing an ANOVA statistical test.

1.3. Results and Discussion

1.3.1. Seasonal Data

Information on irrigation events, season rainfall, and ET_c for 2018 and 2019 are shown in Table 1.3. Rainfall events during crop season for both years were higher than the average (~111 mm) of the last 20 years for crop season (https://hprcc.unl.edu/).

Table 1.3. Seasonal irrigation for full irrigation treatment (100%), rainfall and ET_c data (mm) from the 2018 and 2019 cropping seasons in western Nebraska.

	No. of Irrigation	Irrigation (mm)	Rainfall (mm)	ET_c (mm)
2018	9	151	137	221
2019	12	180	176	274

Total rainfall received were 137 mm and 176 mm during the 90-day DEB growing season of 2018 and 2019, respectively. Cumulative ET_c were 221 mm and 274 mm during the 90-day DEB growing season of 2018 and 2019, respectively (Figure 1.8). In both years, cumulative ET_c were higher than cumulative rainfall.

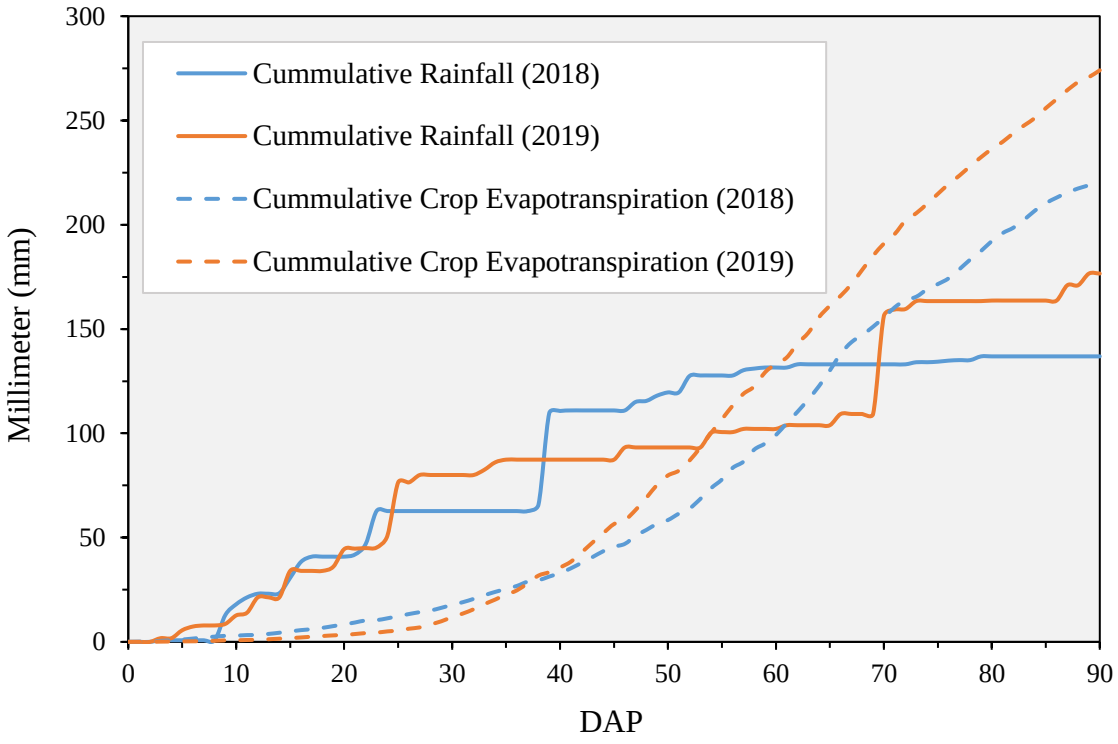

Figure 1.8. Cumulative rainfall and crop evapotranspiration (ET_c) in millimeters (mm) for 2018 and 2019 seasons in western Nebraska. Horizontal axis is represented in days after planting (DAP).

1.3.2. Irrigation treatments and yields

Table 1.4 and Table 1.5 show the irrigation depth (mm) and yields (Mg ha^{-1}) for all irrigation treatments during the two-year study. In 2018, due to heavy rainfall (115 mm) in the first half of season (from 1 to 45 days after planting), irrigation treatments were only divided into two stages, vegetative and reproductive. In 2019, irrigation treatments were divided in the three stages (vegetative, flowering and pod filling). Average yield of all treatments in 2018 was 3.24 ± 0.08 Mg ha^{-1}. This result was similar to yield presented by the dry bean breeding program from the variety trials in Scottsbluff and Mitchell, which was 3.47 Mg ha^{-1} for dry edible bean variety Draco (Urrea and Cruzado, 2018).

In 2019, yields were seven to eight times lower than yields in 2018 (Figure 1.9). The main reason was the research plots were severely damaged by two consecutive hailstorms that occurred on August 14th and August 15th. Dry edible beans were at the pod filling stage (~80% canopy cover) and the crop was not able to fill the pods afterwards due to significant defoliation. After the hailstorm, canopy cover dropped to ~25%. Average yield of all treatments in 2019 was 0.48 ± 0.03 Mg ha^{-1}, which was ~80% lower than the normal average (3.35 Mg ha^{-1}). The breeding program reported values of 2.29 Mg ha^{-1}, however that was only for Mitchell, since hailstorm also damaged the trials in Scottsbluff (Urrea and Cruzado, 2019). Yields were not significantly different among treatments for 2018 (*p-value* = 0.915) and 2019 (*p-value* = 0.950). Figure 1.9 shows the yield variations among the treatments in 2018 and 2019.

Table 1.4. Irrigation amounts (mm) and yields (Mg ha^{-1}) for different irrigation treatments in 2018. Description of treatments represent irrigation amounts applied during vegetative and reproductive stages. Season rainfall (90-day crop season) is also shown in mm.

Treatments	Vegetative-Flowering-Pod Filling	Irrigation (mm)	Season Rainfall (mm)	Yield (Mg ha^{-1})
Treatment 1	0%-0%	12	137	3.12 ± 0.17
Treatment 2	33%-33%	58	137	3.32 ± 0.29
Treatment 3	66%-66%	104	137	3.31 ± 0.29
Treatment 4	100%-100%	151	137	3.16 ± 0.13
Treatment 5	133%-133%	197	137	3.20 ± 0.31
Treatment 6	75%-75%	117	137	3.31 ± 0.32
Treatment 7	50%-100%	138	137	3.20 ± 0.38
Treatment 8	25%-75%	103	137	3.14 ± 0.32
Treatment 9	0%-100%	124	137	3.32 ± 0.29
Treatment 10	0%-100%	124	137	3.15 ± 0.37
Treatment 11	100%-75%	124	137	3.33 ± 0.26
Treatment 12	100%-50%	96	137	3.35 ± 0.20

Table 1.5. Irrigation amounts (mm) and yields (Mg ha^{-1}) for different irrigation treatments in 2019. Description of treatments represent irrigation amounts applied during vegetative and reproductive stages. Season rainfall (90-day crop season) is also shown in mm.

Treatments	Vegetative-Flowering-Pod Filling	Irrigation (mm)	Season Rainfall (mm)	Yield (Mg ha^{-1})
Treatment 1	0%-0%-0%	8	176	0.45 ± 0.13
Treatment 2	33%-33%-33%	65	176	0.49 ± 0.11
Treatment 3	66%-66%-66%	122	176	0.50 ± 0.17
Treatment 4	100%-100%-100%	180	176	0.49 ± 0.17
Treatment 5	133%-133%-133%	236	176	0.44 ± 0.11
Treatment 6	50%-100%-50%	135	176	0.53 ± 0.10
Treatment 7	25%-75%-50%	100	176	0.44 ± 0.09
Treatment 8	100%-0%-0%	21	176	0.50 ± 0.21

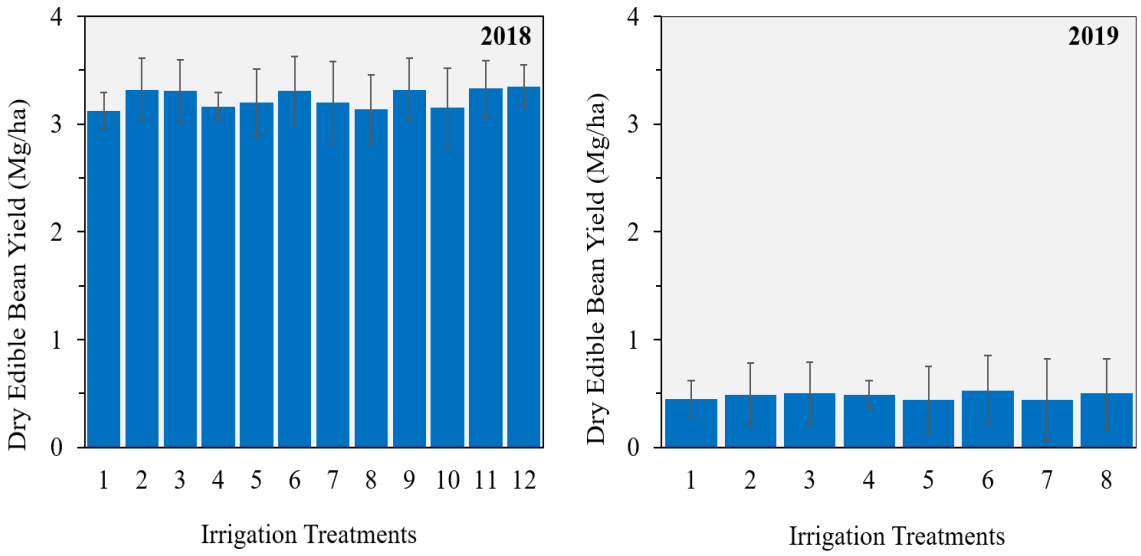

Figure 1.9. Yields in Mg ha^{-1} for 2018 and 2019. X-axis represents irrigation treatments (Table 1.5). The error bars represent one standard deviation of each treatment (n=3).

1.3.3. Soil water monitoring

Figure 1.10 shows the soil water content measured with neutron probe for the different treatments in 2018 at different depths (0 to 120 cm). Figure 1.10 shows that volumetric water content in the topsoil (60 cm) decreases along the season, suggesting the use of the water in the top layer by DEB plants. Contrastingly, volumetric water content below 60 cm does not change along the season, which suggests that DEB roots did not reach or did not actively use the water in those depths.

Figure 1.11 depicts the amount of water in mm per 60 cm depth. In 2018, treatment one and treatment two presented higher soil water amount when compared to soil water amount for treatment four (Figure 1.11), which could be explained by the location of these treatments plots.

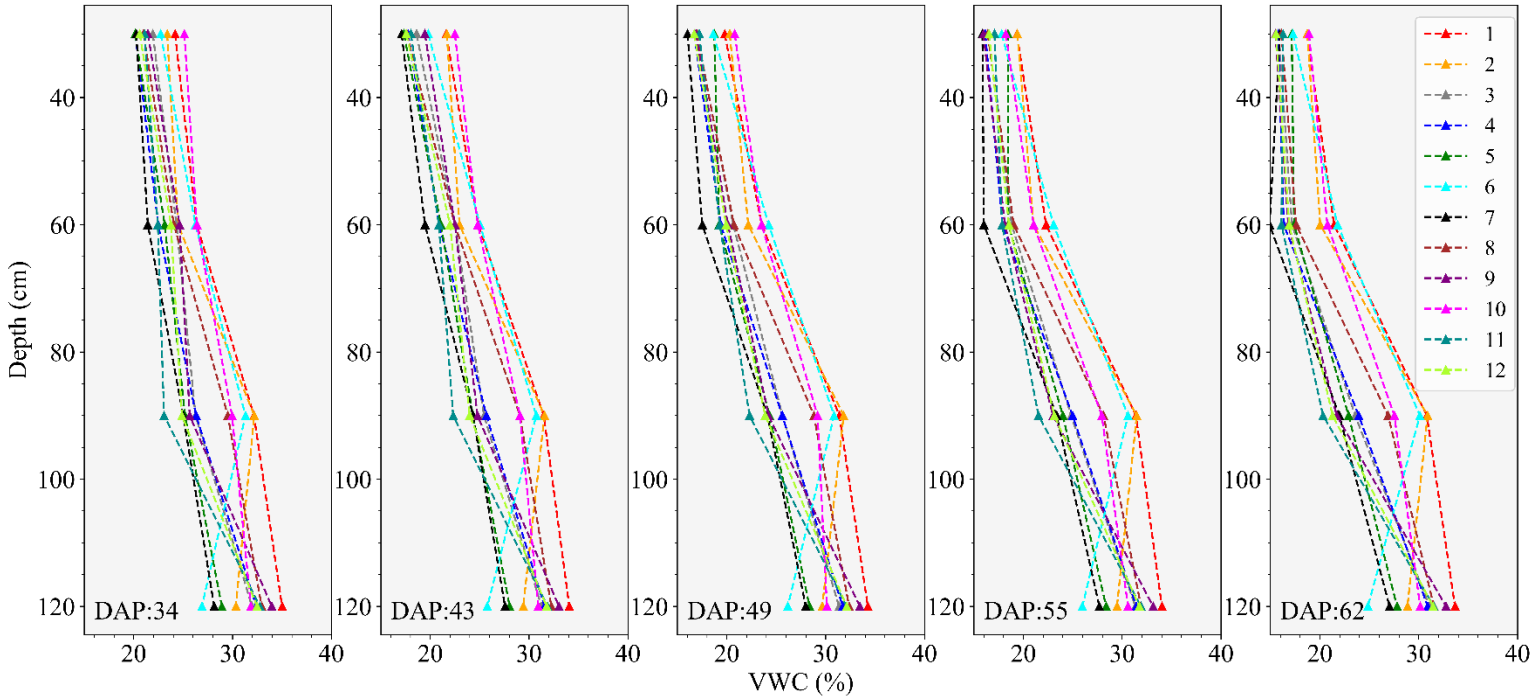

Figure 1.10. Soil volumetric water content (VWC) in percentage of 12 treatments for 5 dates along the season (2018). For details on irrigation treatments, readers should refer to Table 1.5. DAP stands for days after planting.

In 2018, most of the treatment one (0%-0%) plots were located in the southern blocks, where more saturation occurred due to longer standing water during flooding events (Figure 1.2). In addition, during 2018 growing season, the VRI irrigation system was misaligned with the plot design. In short, the plots were designed based on true north and south; however, the linear system moved in an angle, which did not correspond to true north and south. As a result, treatments were overlapping, and it was hard to identify changing of treatment within the plot. Unfortunately, this issue was noticed only after the first three irrigation events in 2018. Therefore, plots did not receive the right amount of water they were designed to receive. This could explain why soil water amount for treatment four was lower than treatment one. Even though, the amount of irrigation application to each plot is unknown, IWUE was calculated for 2018. Values varied from 0.01 to 0.34 Kg m^{-3}, with average of 0.11 ± 0.10 Kg m^{-3}.

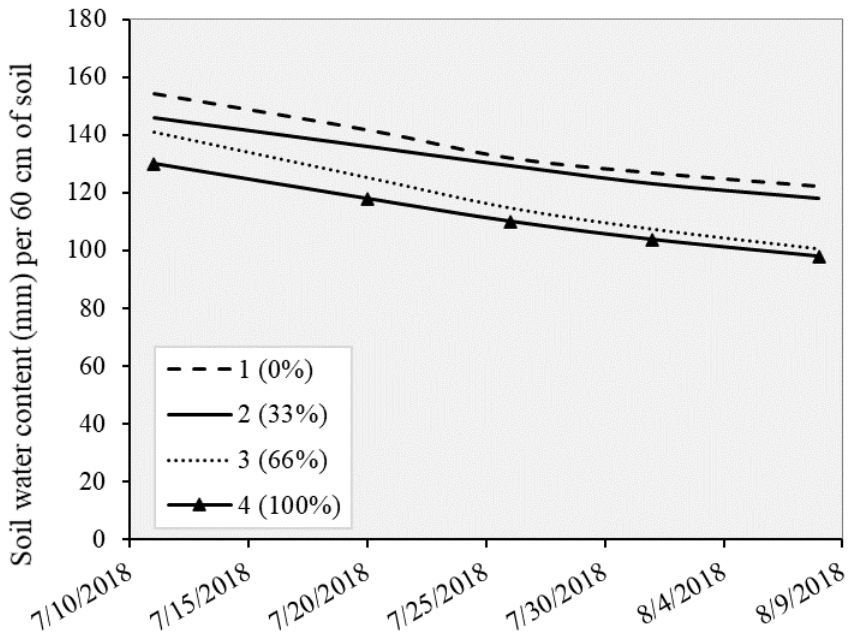

Figure 1.11. Soil water content for treatment 1 (0%-0%), treatment 2 (33%-33%), treatment 3 (66%-66%), and treatment 4 (100%-100%) for 60 cm depth along the season (2018).

Figure 1.12 shows the soil water content measured with neutron probe for 2019. Similar to 2018, soil volumetric water content in the topsoil (60 cm) in 2019 changes along the season, while soil volumetric water content below 60 cm do not show major changes along the season. Also, in 2019, after the 55th day after planting (DAP), soil volumetric water content in the topsoil start to differentiate among the different irrigation treatments, which suggest that irrigation treatments were working. Figure 1.12 shows that treatment one (0%-0%-0%) presents lower soil volumetric water content than treatment four (100%-100%-100%). This difference is most notorious in the topsoil (60 cm), where most of the dry edible bean roots are concentrated.

Figure 1.13 shows amount of water in mm per 60 cm depth. For the 2019 season, the amount of water in soil for the different treatments followed the expected distribution (higher amounts for treatment four and lower amounts for treatment one), but due to the hailstorms, yields were severely affected, thus they were not representative of their respective irrigation treatment. Consequently, IWUE was not calculated for 2019.

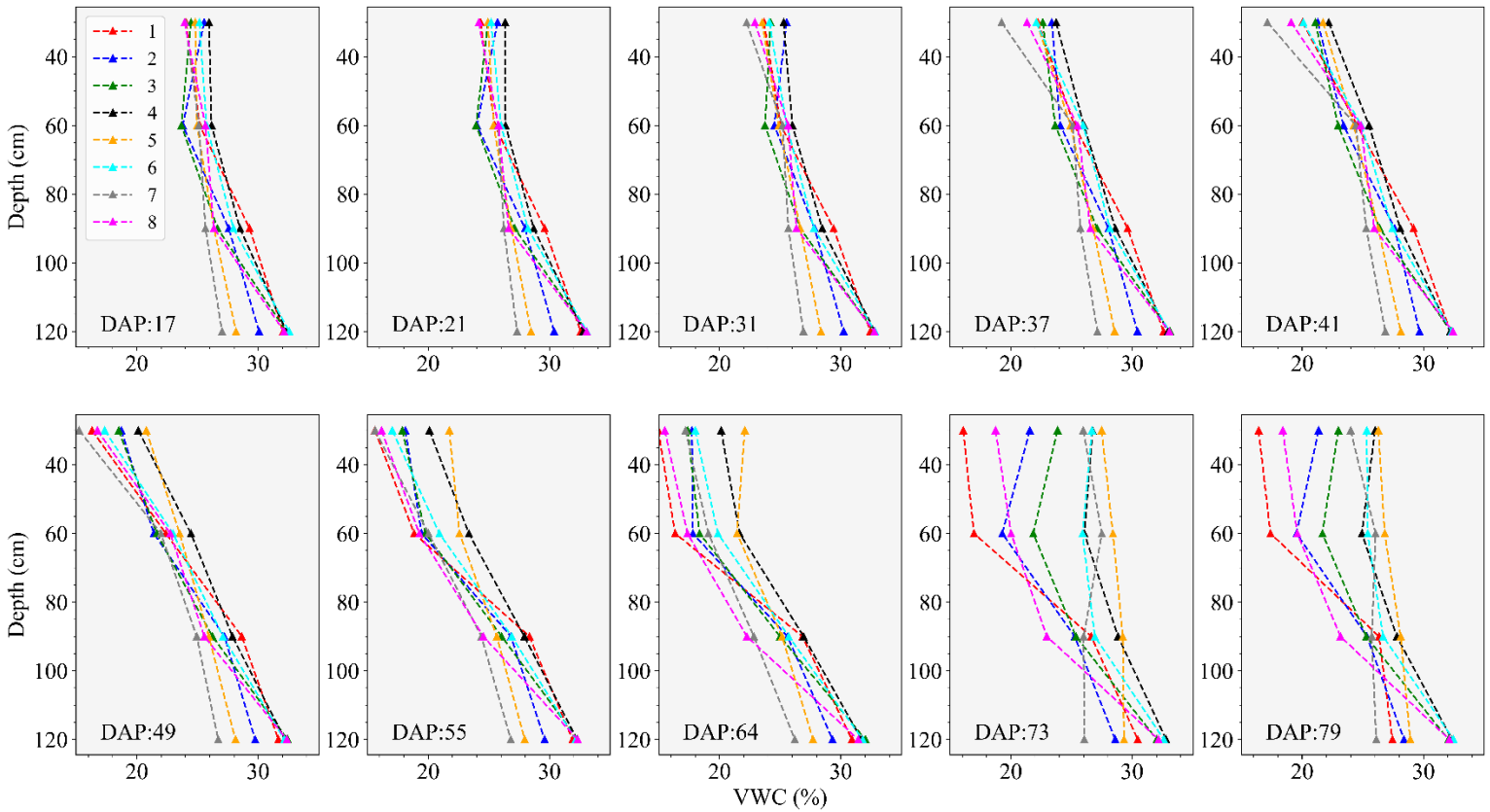

Figure 1.12. Soil volumetric water content (VWC) in percentage of 8 treatments for 10 dates along the season (2019). For details on irrigation treatments, readers should refer to Table 1.6. Hailstorm took place on the 65th day after planting (DAP).

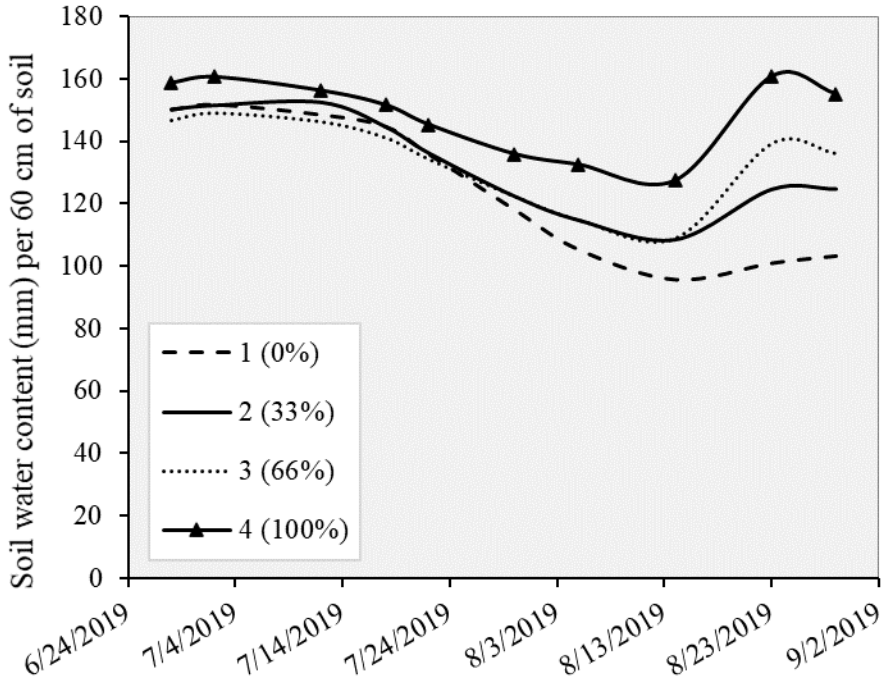

Figure 1.13. Soil water content for treatment 1 (0%), treatment 2 (33%), treatment 3 (66%) and treatment 4 (100%) for 60 cm depth along the season (2019).

Figure 1.14 depicts the drone images taken along the 2019 season, which shows the damage caused by the hailstorms. The left image (Figure 1.14 A) (August 8th) was taken before the hailstorms and it shows the differences among the irrigation treatments. The plots' canopies were greener and denser for plots that received a higher irrigation treatment (i.e. treatment four), especially when compared to treatments that received less water (i.e. treatment one). The middle image (Figure 1.14 B) (August 16th) was taken a couple days after the hailstorms. Though the irrigation plots were still green, since hailstorm had just happened two days earlier, it is harder to visually differentiate the irrigation treatments. The right image (Figure 1.14 C) (August 28th), shows the irrigation plots 14 days after the hailstorm. From this picture, it is possible to observe that the plants were defoliated and became completely brown.

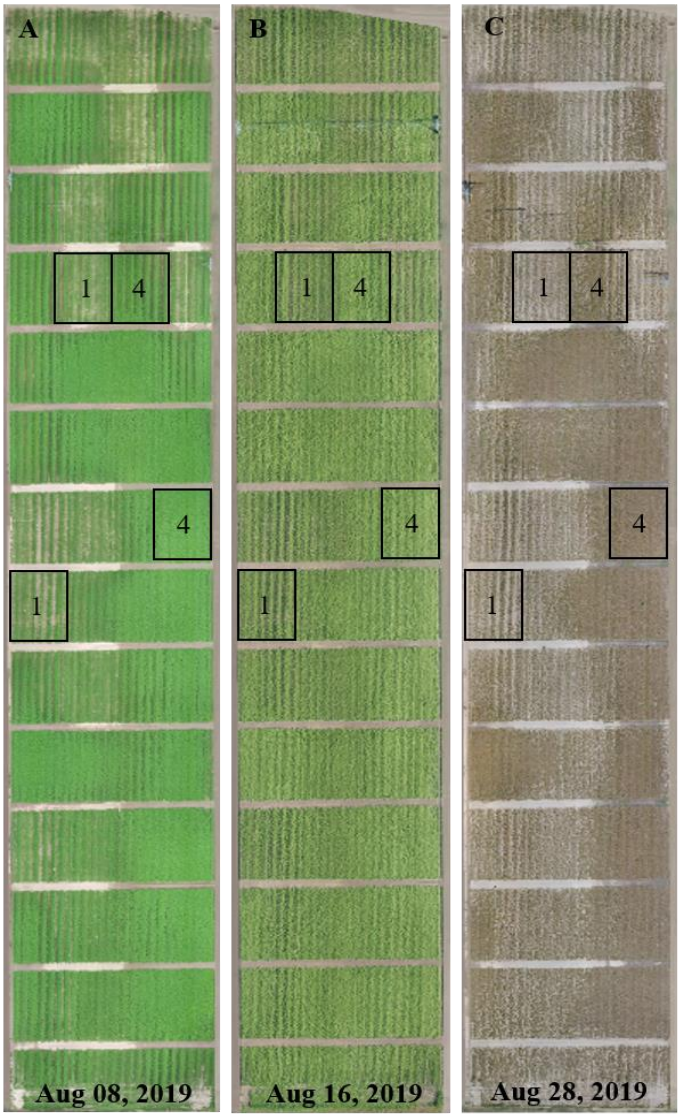

Figure 1.14. Images captured with drone. Left image (A, August 8th, 2019) was taken before hailstorms; middle image (B, August 16th, 2019) was taken two days after hailstorms; and right image (C, August 28th, 2019) was taken two weeks after hailstorms. Plots with treatment 1 (0%-0%-0%) and treatment 4 (100%-100%-100%) are represented in images.

1.4. Conclusion

This study aimed to evaluate DEB yield at different deficit and limited irrigation scenarios. In 2018, yields varied from 3.12 Mg ha^{-1} to 3.35 Mg ha^{-1} with average of 3.24 ± 0.08 Mg ha^{-1}, and IWUE varied from 0.01 to 0.34 Kg m^{-3}, with average of 0.11 ± 0.10

Kg m^{-3}. In 2019, yields varied from 0.44 to 0.53 Mg ha^{-1}, which was ~80% lower than the normal average (3.35 Mg ha^{-1}). Yields were much lower due to two hailstorms that occurred during DEB pod filling stages. Since yields were not representative of irrigation treatments, IWUE was not calculated for 2019.

CHAPTER 2. DEVELOPMENT AND EVALUATION OF CROP WATER STRESS INDEX FOR VARIOUS IRRIGATION TREATMENTS OF DRY EDIBLE BEANS IN WESTERN NEBRASKA

Abstract

Infrared radiometry thermometer (IRT) is a well-established tool used for water stress estimation and irrigation management. The IRT measures crop canopy temperature, which can be used to calculate an empirical crop water stress index (CWSI) to assess plant water stress. The index varies from zero (well-watered crop) to one (water stressed crop). Though there have been several studies using IRT and CWSI to assess plant water stress of many crops (e.g. corn and soybeans), there is a lack of studies evaluating the feasibility of this approach to measure crop water stress on dry edible beans (DEB). The aim of this study is twofold. First, to calculate CWSI baseline equations for DEB in western Nebraska. Second, to calculate and compare CWSI values for different irrigation treatments and to verify if canopy temperature and CWSI techniques can be used to quantify water stress in DEB. To obtain the baselines, IRTs were installed on DEB fields at four irrigation treatments (0%, 33%, 66% and 100% of fully irrigated crop evapotranspiration (ET_c)) during the 2018 and 2019 growing seasons. Lower CWSI baselines were determined using data from fully irrigated plots (100% irrigation) and upper CWSI baselines from rainfed plots (0% irrigation). The main factors used to calculate baselines were vapor pressure deficit (VPD), canopy temperature (T_c) and air temperature (T_a). The average lower baseline found for both years was $T_c - T_a = 2.78 - 1.59$ VPD ($n = 25$, $R^2 = 0.81$) and upper baseline was $T_c - T_a = 3.76$ ($n = 11$, $SD = 0.42$). By plotting CWSI values along the growing seasons, differences between CWSI values

from different irrigation treatments were observed, specially between 12:00 PM and 3:00 PM during daily peak water demand; treatments with higher irrigation rates presented lower CWSI (close to zero) and treatments with lower irrigation rates presented higher CWSI (close to one). Even though the CWSI optimum value to trigger irrigation was not determined in this study, the differences in CWSI values among the different irrigation treatments suggest that this method has a potential use in irrigation scheduling for DEB in western Nebraska.

2.1 Introduction

Martin et al. (1990) classified irrigation scheduling into two groups: 1) soil water balance approach, and 2) soil and/or crop monitoring techniques. The soil water balance approach relies on quantifying soil water storage change by calculating all basic elements of the water balance: crop evapotranspiration (ET_c), deep percolation, runoff, irrigation and precipitation. The key to success of this approach is the accurate quantification of ET_c, which can be calculated using different methods: Pan method (Ucar et al., 2009), FAO 56 Penman-Monteith crop coefficient approach (Medeiros et al., 2005), and weighing lysimeter (Medeiros et al., 2001). The FAO 56 (Allen et al., 1998) is the prevailing method and it is widely accepted due to its easiness to implement, since it scales a Penman-Monteith reference ET (ET_o or ET_r) with crop coefficients. However, the application of this method at farm scale is very limited, as it depends on accurate estimates of ET_o, which requires daily collection of weather information in some proximity to the site. Currently, most farmers do not have an accurate method to measure daily plant water use, therefore introducing uncertainties when estimating ET_c. Moreover, the soil water balance approach tends to drift off-target and build accumulated error if

wrong initial soil water conditions are used or any component required to compute soil water change is missing, such as the soil water holding capacity. Therefore, soil water balance approach should only be used if initial soil water content and the available water capacity of the soil are known, and if farmers have a precise method to measure ET_c and precipitation (Andales and Chávez, 2011).

Under these circumstances, on-site monitoring is necessary for precise irrigation scheduling, which mostly applies to the second irrigation scheduling group: soil and/or crop monitoring techniques. On-site soil moisture sensing using reflectometry, capacitance probes, electrical resistivity measurements and telemetry technology has gained popularity during the past decades, especially after Topp et al. (1980) introduced a laboratory approach to measure volumetric water content (θ_v) using electromagnetic signals to determine the dependence of the dielectric constant (K) on θ_v. The USDA's Farm and Ranch Irrigation Survey (FRIS) report showed that there were 4413 (29.8%) farms using daily data of ET_c and 2019 (14.2%) using soil moisture devices for irrigation scheduling in Nebraska (USDA FRIS, 2008). A more recent survey showed that the adoption rate of ET_c method dropped ~5% and it increased ~7% for soil moisture sensing devices (USDA FRIS, 2013). The increasing adoption rate of soil moisture sensor-based irrigation scheduling indicates the farmers' growing interest in this method. In addition, cost share programs provided by the Natural Resources Districts (NRDs) have offset certain amount of the high expenses of soil moisture sensing devices (Rudnick et al., 2015) and made it more accessible to farmers in Nebraska.

Although soil moisture sensing devices are popular and serve as a base for irrigation scheduling, it is still an indirect scheduling tool that does not take into account

the immediate plant water status. Plant water stress may be a result of a combination of multiple factors, such as: environmental conditions (air temperature, relative humidity, solar radiation intensity), light interception (canopy cover), and root condition (access to available water in the soil). In other words, available water in the root zone, which is measured by soil moisture sensors, is not always directly correlated with the water status of the plant. Leaf water potential is one of the direct methods used to measure plant water status, however the necessity of plant contact and destructive sampling make it difficult for farming operations. This might be the reason of low adoption rate (<1%) of plant based irrigation scheduling in NE according to USDA FRIS (2013).

One of the most popular methods used for crop monitoring was first presented by Jackson et al. (1977). The researchers introduced a non-contact method to detect plant water stress based on canopy temperature measured by infrared radiometry. Later, a canopy temperature-based water stress indicator named Crop Water Stress Index (CWSI) was developed (Idso et al., 1981) to quantify plant water stress using data from infrared radiometers. This index varies from zero to one, where zero represents a well-watered crop and one represents a severely water-stressed crop. The empirical form of CWSI is calculated based on three main variables: plant canopy temperature (T_c), air temperature (T_a), and vapor pressure deficit (VPD). This index has been tested under different environmental conditions, for example, sub-humid subtropical (Gontia and Tiwari, 2008) and semi-arid (Erdem et al., 2006; Irmak et al., 2000; da Silva and Rao, 2005). Previous research showed that CWSI performs best in arid and semi-arid climates (Jones, 1999), partially due to smaller variabilities of factors that affect CWSI calculation (e.g. wind speed, canopy surface roughness and net radiation) in arid/semi-arid climate compared to

humid climate (Hipps et al., 1985; Jones, 1999). In addition, humid areas, such as maritime climates, tend to have more clouds, which affects the canopy temperature readings (Jones, 1999).

Crop water stress index was also tested as an irrigation management method for several crops, for example, maize – (*Zea Mays* L.) (Irmak et al., 2000; Taghvaeian et al., 2012), cotton – *Gossypium hirsutum* L. (Pinter and Reginato, 1982; da Silva and Rao, 2005), and soybean – *Glycine max* L. (Nielsen, 1990), but there is a limited amount of research with CWSI for DEB (Erdem et al., 2006; Asemanrafat and Honar, 2017). CWSI has been compared with other plant water stress indicators, for example, volumetric water content (VWC) in top soil (Taghvaeian et al., 2012), and xylem pressure potential of leaves (ψ_l) (Pinter and Reginato, 1982, DeJonge et al., 2015). Taghvaeian et al., (2012) showed there was a strong linear relationship ($R^2 = 0.89$) between CWSI and VWC in topsoil by using a second order polynomial equation ($VWC = 6.63\ CWSI^2 - 12.76\ CWSI + 28.31$). Pinter and Reginato (1982) showed that CWSI alone did not have a strong agreement ($R^2 = 0.45$) to xylem pressure potential of leaves, however when plant age and VPD were added to equation ($\psi_l = -0.274 - 0.905\ CWSI - 0.010\ age - 0.19\ VPD$), the relationship was stronger ($R^2 = 0.76$). DeJonge et al. (2015) showed that midday xylem pressure potential of leaves (ψ_l) was highly correlated ($R^2 = 0.89$) to canopy temperature at midday, proving that canopy temperature and its subsequent thermal indices can be used to quantify water stress. Irmak et al. (2000), da Silva and Rao (2005) and Nielsen (1990) focused on determining an optimum CWSI value to trigger irrigation by using different methods; authors associated CWSI with yields (Irmak et al., 2000), calculated the average well-watered crop CWSI value along the season (da Silva and Rao, 2005)

and selected certain values to trigger irrigation and afterwards compared yields among treatments (Nielsen, 1990). Irmak et al. (2000) found CWSI values higher than 0.22 led to a decrease in yield for maize. Yet the authors affirm that the value should not be used to schedule irrigation, since it was not tested for irrigation scheduling in their experiment. For cotton, da Silva and Rao (2005) found the optimum CWSI of less than 0.3, however authors describe the difficulties in determining that value due to large variability in variables such as solar radiation, air temperature, wind speed and VPD, which influences canopy temperatures. For soybeans, Nielsen (1990) found the optimum value by testing irrigation scheduling using thresholds of 0.2, 0.3, 0.4 and 0.5. Yields for different irrigation treatments were compared and authors concluded that CWSI values should not exceed 0.2.

Crop water stress index is calculated using two baselines: lower and upper baselines. The lower baseline, also known as the non-water stressed baseline can be determined following procedure described by Gardner et al. (1992b) by fitting difference of canopy of non-water stressed crop (fully irrigated) and air temperature (dT_{LL}) to corresponding vapor pressure deficit (VPD), as shown in Equation 1:

$$dT_{LL} = \mathrm{m} \times VPD + b \quad (1)$$

Where *m* is the slope of linear equation; *b* is the intercept of linear equation; and VPD is vapor pressure deficit (kPa).

Vapor pressure deficit (VPD) can be determined by following equations presented by Allen et al. (1998):

$$e_s = 0.6108 \times \exp\left[17.27\frac{T}{T+237.3}\right] \quad (2)$$

$$e_a = e_s \times \left(\frac{RH}{100}\right) \quad (3)$$

$$VPD = e_s - e_a \quad (4)$$

Where e_s is saturation vapor pressure (kPa); e_a is the actual vapor pressure (kPa); and T is the mean air temperature (^{o}C).

The upper baseline, also known as non-transpiring baseline, can be calculated using canopy temperature of rainfed crop. In general, the upper baseline is often presented as a constant value for difference of canopy and air temperature regardless of VPD values at the time (Irmak et al., 2000; Erdem et al., 2006; Taghvaeian et al., 2014). According to Idso et al. (1981), the upper baseline is a function of air temperature with small variations along the VPD axis. Therefore, using a constant value for the upper baseline introduces small uncertainties (Gardner et al., 1992a). Average of temperature difference between canopy and air at non-transpiring plots (dT_{UL}) values are used to calculate the upper baseline.

Gardner et al. (1992a) stated that multiple baselines along the season are needed due to change in water need at different crop stages. Yet several studies have successfully implemented CWSI by utilizing the same baselines throughout the season (Idso et al., 1981; Irmak et al., 2000; DeJonge et al., 2015). It is also worth noting that CWSI baseline varies for different locations and different crops. An example is shown in Figure 2.1, which presents multiple lower baselines determined for maize at various locations: Idso (1982) – Tempe, AZ, USA; Nielsen and Gardner (1987) – Akron, CO, USA; Yazar et al. (1999) – Busland, TX, USA; Irmak et al. (2000) – Antalya, Turkey; DeJonge et al. (2015)

– Greeley, CO, USA; Han et al. (2018) – Greeley, CO, USA. Figure 2.1 shows that there are baselines variations even for the same crop and location (DeJonge et al., 2015 and Han et al., 2018). Therefore, collecting in-situ data to develop baselines based on local conditions is essential before using CWSI to monitor plant water stress (Nielsen, 1990; Gardner et al., 1992a).

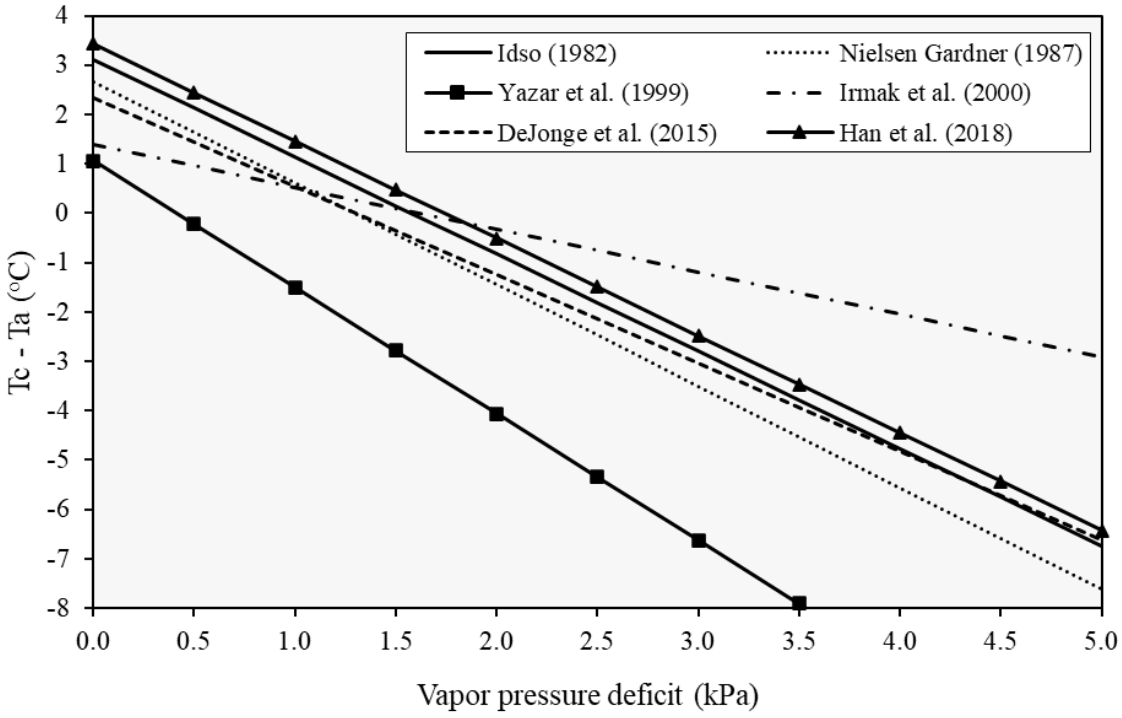

Figure 2.1. Lower baselines of crop water stress index (CWSI) reported by different researchers for maize.

Some other drawbacks of using CWSI as an irrigation tool include: (1) the index can be used for identifying timing of irrigation rather than amount of irrigation and (2) CWSI values can be overestimated during early stage of crop development, since canopy temperature readings are influenced by the bare soil. Some studies proposed using CWSI only after the canopy cover reached 100% (Irmak et al., 2000) or at least 80% (DeJonge

et al., 2015). Regardless of the limitations when using CWSI, it is still well accepted by most researchers and can be a valuable tool for farmers when managing irrigation.

As described above, CWSI has been applied to several crops. However, to our knowledge, there have been limited attempts to implement CWSI as a tool to monitor crop water stress on DEB. Therefore, our objectives were to: 1) develop CWSI baselines for DEB in western Nebraska; and 2) evaluate the response of CWSI for DEB at different irrigation treatments.

2.2 Material and Methods

2.2.1 Study location and experimental design

The experiment was conducted at the University of Nebraska Lincoln Panhandle Research and Extension Center (PHREC) in Scottsbluff, NE (41°53'34.93"N, 103°41'2.04"W, elevation 1189 m). For site information and irrigation treatments, readers are suggested to refer to Chapter 1. In Chapter 2, a subset of irrigation treatments from Chapter 1 is used. The treatments are Treatment 1 (0%-0%-0%), Treatment 2 (33%-33%-33%), Treatment 3 (66%-66%-66%), and Treatment 4 (100%-100%-100%). Irrigation treatments are represented in percentage of full plant water need.

2.2.2 Canopy temperature measurements

Canopy temperature was measured using Infrared Thermometer (IRT) from Apogee Instruments (Model: SI-431, SDI12 output Apogee Instruments, Inc., Logan, Utah, USA). The particular IRT model has a field of view of 14° half angle with accuracy of ± 0.3 °C for temperature range of -10 to 65 °C. IRTs were installed at three

replications for each irrigation treatment. IRTs were mounted to a bracket on a galvanized pole (1.8 m high with 4.12 cm in diameter) at 1.2 meters above ground and were angled 45 degrees below horizon and parallel with the crop row (Figure 2.2). Sensor was set up parallel to the crop row in order to make it easier to estimate area seen by sensor and account for factors that could influence the temperature recorded by IRT, i.e. soil and missing plant. Heights of IRTs were kept the same throughout the season. The total area seen by the sensor varied from 0.88 m^2 when plants had just emerged to 0.26 m^2 once plants were fully developed and plant height was 0.65 cm. The areas were calculated based on the height from sensor to the view surface and angle of the sensor (https://www.apogeeinstruments.com/irr-calculators/). Sensors were installed on July 6th, 2018 and July 15th, 2019. Dry edible beans were at stages V2/V3 when sensors were installed. Figure 2.3 shows a set up example of an IRT.

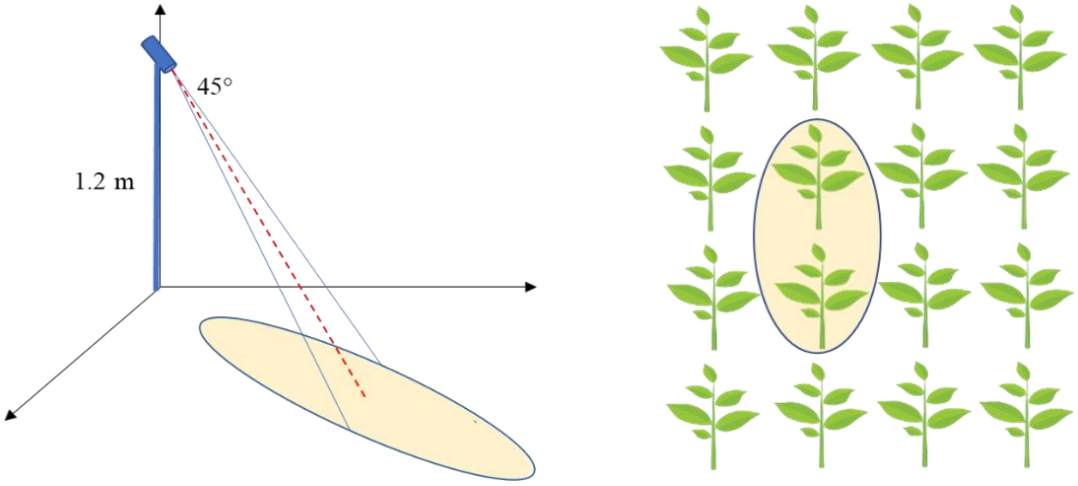

Figure 2.2. On the left, footprint seen by the IRT. On the right, area seen by IRT in the field, which was angled parallel with crop rows.

Figure 2.3. Set up for IRT located in the middle rows of an irrigation plot.

Data from the sensors were continuously recorded using data loggers (CR300, Campbell Scientific Inc., Logan, Utah, USA) every 30 minutes in 2018 and every 5 minutes in 2019. The data logger programming code is found in Appendix A. The data was manually downloaded every week from data loggers. Locations of data loggers and IRT shown in plot maps in Figure 2.4.

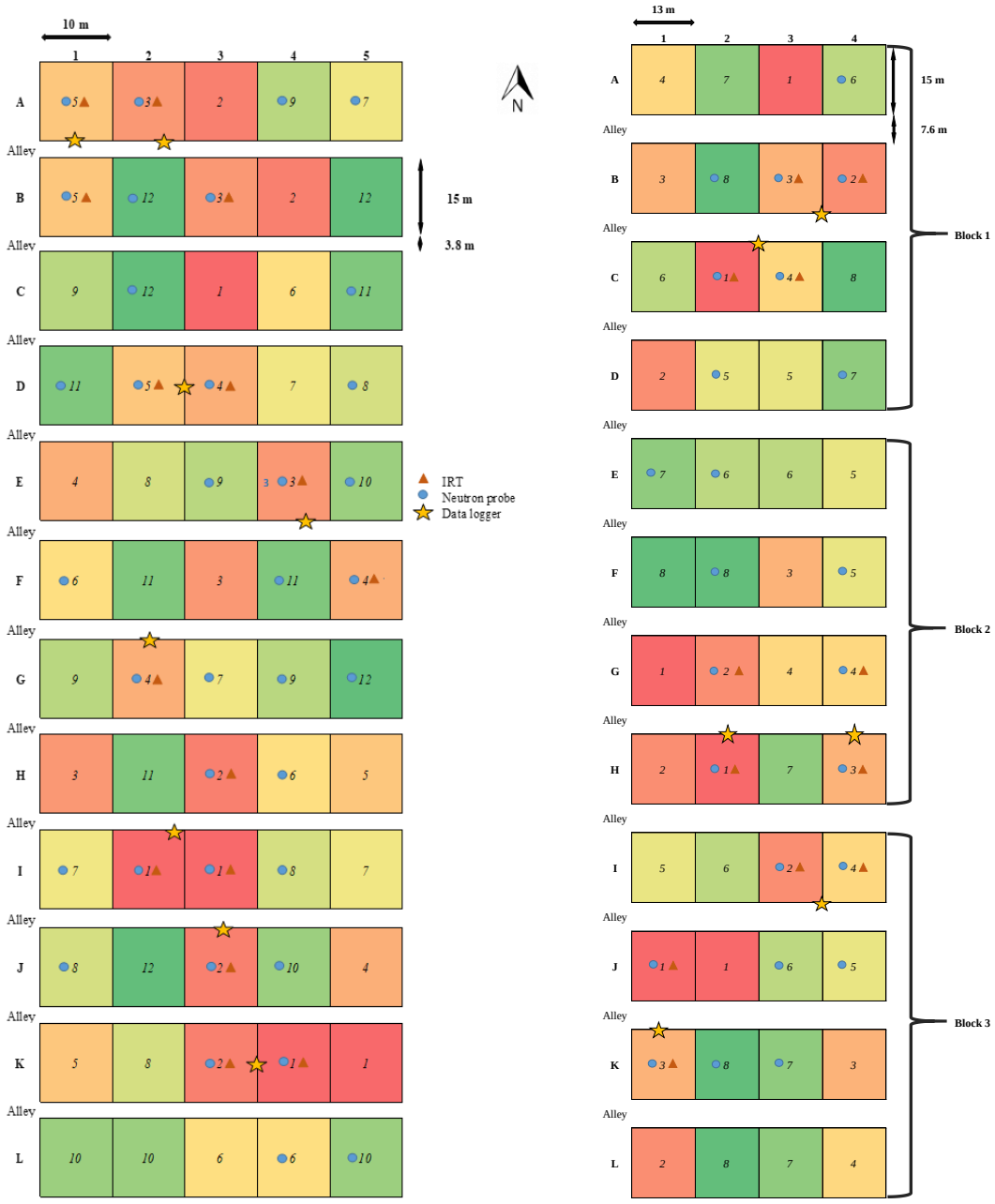

Figure 2.4. Plot maps and sensor location for 2018 (left) and 2019 (right). Numbers inside plots represent different irrigation treatments. For more details on irrigation treatments, readers should refer back to Chapter 1.

Each data logger was powered by a solar panel (10M-V, Peak Power – Pmax: 10 W, voltage at Pmax: 18.1 V, current at Pmax: 0.55 A, Ameresco Solar) and a 12 volt battery (Genesis NP0.8-12 12V/0.8AH Sealed Lead Acid Battery with JST Wire

Terminal). Solar panel was set facing south and with a 45^{o} degree angle from horizon. Waterproof data logger enclosures from Bud Industries Inc. (Willoughby, Ohio, USA) were used in this experiment. Some modifications were made to the enclosure to be able to hold the necessary instruments, such as, battery and data logger (Figure 2.5 A). Each enclosure contained one data logger, one battery and eight openings with water-tight cable glands to be able to insert sensor cables. Figure 2.5 B shows the wiring of sensors. Both data logger enclosure and solar panel were attached to a galvanized pole 2.4 m high and with 6 cm in diameter. There was a total of eight data loggers in 2018 and six in 2019.

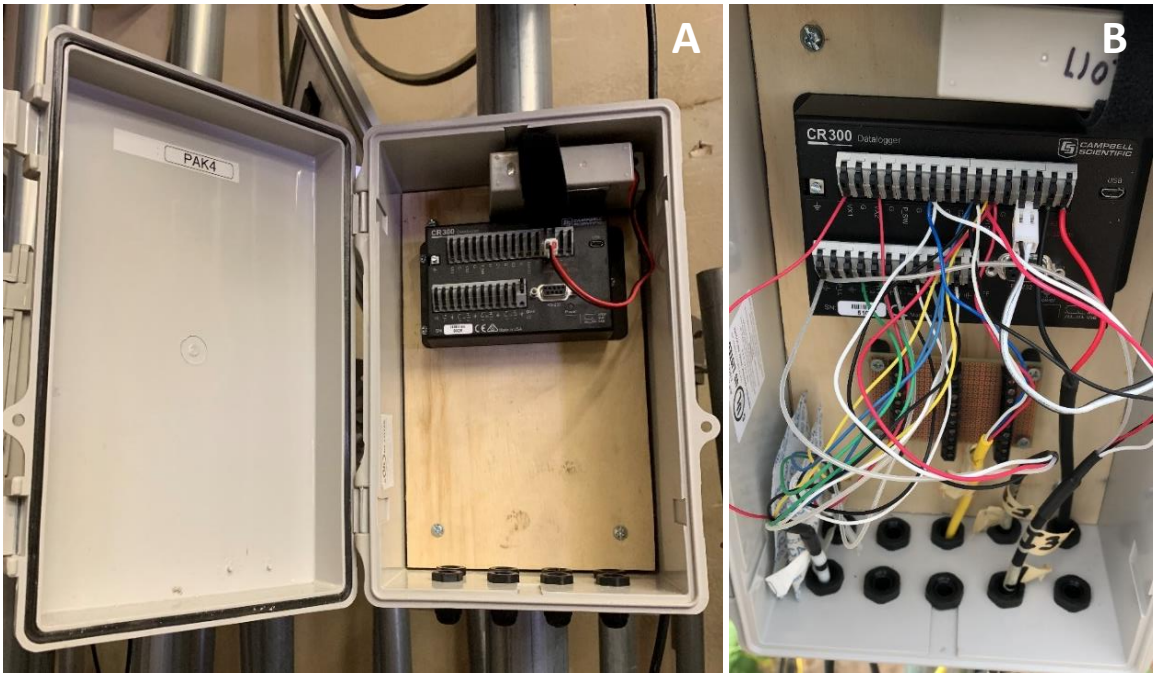

Figure 2.5. Data logger enclosure adapted for this experiment (A); wiring of sensors (B).

2.2.3 Other measurements

In order to monitor the differences across the irrigation treatments, other measurements were taken along the seasons. One of them was soil water monitoring, which was done on weekly basis at four depths (30, 60, 90, and 120 cm) using a neutron probe (CPN 503 DR Hydroprobe, Concord, CA, USA). Readers should refer to chapter 1 for more details.

Another measurement taken along the season was leaf stomatal conductance, which is a well-known method used to monitor crop evapotranspiration. Leaf stomatal conductance was recorded for both seasons (2018 and 2019) using leaf porometer (Decagon Devices, Inc., Pullman, WA, USA) (Figure 2.6) for all four treatments. A total of three values was recorded for each plot and there were three repetitions for each treatment. Readings were taken from top leaves and during open sky conditions (no clouds) between 11:00 AM and 2:00 PM. The reading process of a porometer requires plant leaves surface to be dry, therefore, rainy and irrigation days and first day post irrigation were avoided. Calibration was done at the beginning of each day following the steps presented by the device's manual.

Figure 2.6. Leaf porometer used in this experiment (Decagon Device Inc. Leaf Porometer Manual, 2016).

In 2019, leaf area index (LAI) were taken using a plant canopy analyzer (LAI-2200C, LI-COR Environmental, Lincoln, NE, USA). The sensor consists of two parts, the console and the optical sensor, as seen in Figure 2.7. The console is where all the setup is done and where data is stored. The optical sensor is where the fisheye lens with hemispheric field-of-view is located and where readings are taken from. The plant canopy analyzer uses the gap fraction method to calculate LAI, which consists of measuring the interception of blue light going through the canopy. The plant canopy analyzer takes readings using five silicon detectors arranged in concentric rings, as seen in Figure 2.8, which allows measuring light from five different zenith angles with one reading (LI-COR Plant Canopy Analyzer Manual, 2016).

Figure 2.7. LAI-2200C Plant Canopy Analyzer (optical sensor, left; console, right) (LI-COR Plant Canopy Analyzer Manual, 2016).

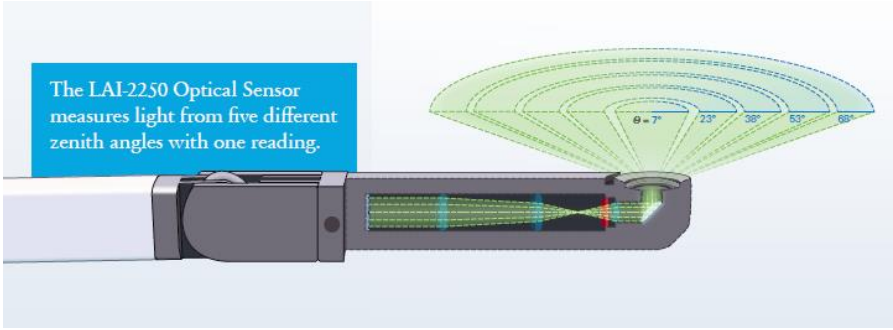

Figure 2.8. Five angles used to measure light interception (LI-COR Plant Canopy Analyzer Manual, 2016).

Five view restricting caps were provided with the LAI-2200C. Different angle openings are used in order to minimize error caused by measuring of undesired surroundings, for example, the operator. In this study, a 45^{o} view cap was used, as suggested in the manual for readings in row crops.

To measure LAI at each plot, there were six LAI readings including one above the canopy (for reference) and five below the canopy. The five below canopy readings were taken moving from one crop row to adjacent crop row, as shown in Figure 2.9. Above canopy readings were taken at about one meter above the ground, and below canopy readings were taken close to the ground.

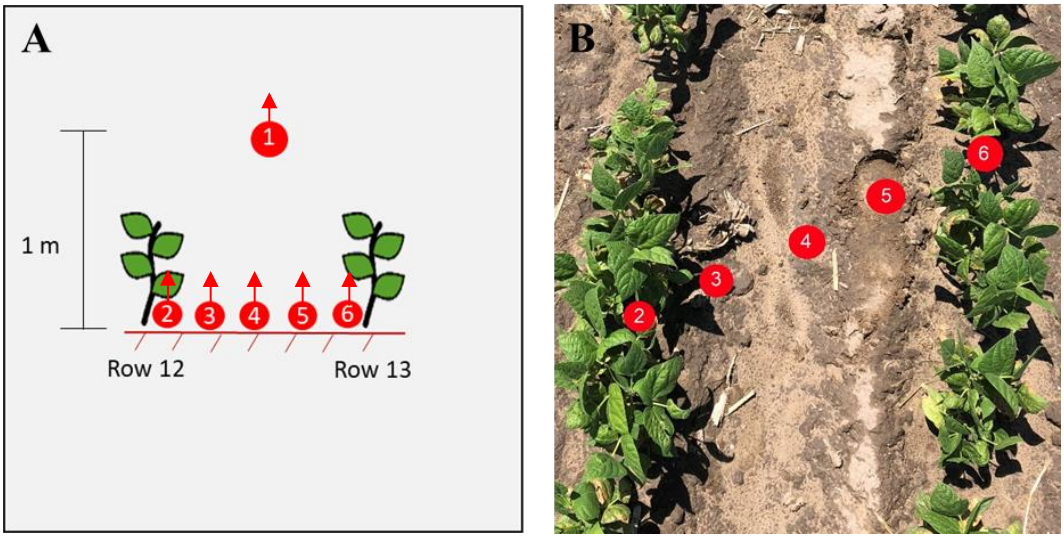

Figure 2.9. Representation of where LAI readings were taken. (A) sectional view and (B) bird's-eye view. Red arrows on image A represent direction sensor is pointed to.

2.2.4 Calculation of CWSI

2.2.4.1 Baselines

Because CWSI baselines require specific types of data, the data retrieved from IRTs were filtered for clear sky solar radiation and dry leaves before the calculation of baselines. Gardner et al. (1992b) reported several factors that could affect CWSI values (e.g. rainfall/irrigation events, wind speed, and time of IRT readings). In this study, four steps were taken to filter the data to calculate the baselines. The first was exclusion of data for days with irrigation/rainfall events and the second was exclusion of data on

cloudy days. The third filter was selection of the time; only data between 1:00 PM and 2:00 PM was selected to develop baselines to focus on times that would experience maximal water stress. At last, the fourth filter applied was on canopy cover; IRTs readings taken before the canopy cover reached 80% were not considered to minimize bias from bare soil. Once all the data had been filtered, upper and lower baselines were calculated, following methods described previously in introduction.

In order to determine a cloudy day, relative shortwave radiation (R_s/R_{so}, where R_s is solar radiation and R_{so} is clear-sky solar radiation) was used. The ratio varies between about 0.33 (dense cloud cover) and 1 (clear sky) (Allen et al., 1998). Therefore, in this study if ratio was below 0.6, data was excluded from baseline calculation.

Calculations of R_s and R_{so} were done following the method presented on Chapter 3 of FAO-56 (Allen et al., 1998). The following equations were used:

$$R_s = \left(a_s + b_s \frac{n}{N}\right) R_a \tag{5}$$

where R_s is solar or shortwave radiation (MJ m^{-2} day^{-1}), a_s and b_s are Angstrom values (if no calibration has been carried out in the area for improved a_s and b_s parameters, the values used should be $a_s = 0.25$ and $b_s = 0.50$), n is the actual duration of sunshine (hour), N maximum possible duration of sunshine or daylight hours (hour) and R_a extraterrestrial radiation (MJ m^{-2} day^{-1}).

$$R_{so} = (0.75 + 2\ 10^{-5}\ z)R_a \tag{6}$$

where z station elevation above sea level (m).

Daily extraterrestrial radiation (Ra) can be calculated following Equation 7:

$$R_a = \frac{1440}{\pi}\, G_{sc}\, d_r \times\, [\omega_s \sin(\varphi) \sin(\delta) + \cos(\varphi) \cos(\delta) \sin\,(\omega_s)] \quad (7)$$

where R_a is the extraterrestrial radiation in the hour (or shorter) period (MJ m^{-2} $hour^{-1}$), G_{sc} is the solar constant = 0.0820 MJ m^{-2} min^{-1}, d_r is the inverse relative distance Earth-Sun, δ is solar declination (rad), ω_s is the sunset hour angle (rad) and φ is latitude (rad).

$$d_r = 1 + 0.033cos\left(\frac{2\pi J}{365}\right) \quad (8)$$

where J is Julian day of the year (1 to 366).

$$\delta = 0.4093\, sin\left(\frac{2\pi(284 + J)}{365}\right) \quad (9)$$

$$\omega_s = arccos(\Psi) \quad (10)$$

$$\Psi = \tan(\varphi)\, tan(\delta) \quad (11)$$

2.2.4.2 CWSI values

CWSI was calculated using empirical formula proposed by Idso et al. (1981):

$$CWSI = \frac{(dT_m - dT_{LL})}{(dT_{UL} - dT_{LL})} \quad (12)$$

Where dT is the difference between canopy and air temperature (°C); *m* denotes the measured difference between canopy and air temperature; LL denotes the lower limits (lower baseline); and UL is for the upper limits (upper baseline).

A local sensitivity analysis was performed to determine which component of CWSI calculation – upper baseline, lower baseline slope or lower baseline intercept – contributed the most to changes in CWSI values. Values for slope and intercept of lower

baseline varied from -0.79 to -2.39 and from 1.98 to 3.58, respectively; and values for upper baseline varied from 2.96 to 4.56. Baseline scenarios used for the sensitivity analysis were the parameters found for the average lower and upper baselines. Values for the three parameters varied in 0.2 ^{o}C increments from their baseline scenario.

2.3 Results and Discussion

2.3.1 Weather and yield data

Season rainfall, ET_c and yield data for the different irrigation treatments are available in section 1.3 in chapter 1. For details, readers should refer to the previous chapter.

2.3.2 Leaf Porometer

Figure 2.10 depicts the average stomatal conductance (SC) (mmol $m^{-2}s^{-1}$) measured using the leaf porometer during 2018 and 2019 growing seasons for all treatments.

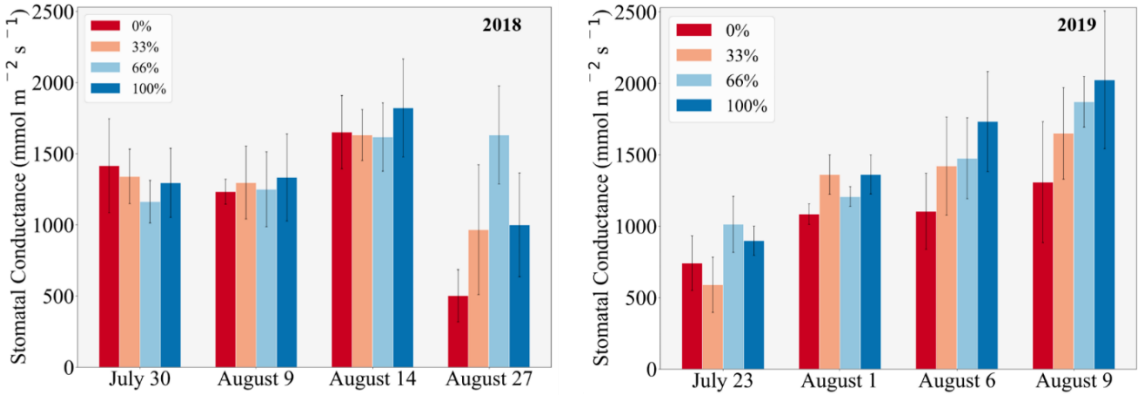

Figure 2.10. Stomatal conductance for four different dates during the 2018 (left) and 2019 (right) growing seasons. Different colors represent different irrigation treatments. The error bars represent one standard deviation of each treatment (n=3).

Figure 2.10 (2018) shows that during the 2018 growing season, average SC were not significantly different among irrigation treatments (*p-value* = 0.85). Treatments do not show the expected increase in SC with increasing applied irrigation. However, a different behavior is observed during 2019 growing season, where SC was significantly different among treatments in 2019 (*p-value* = 0.01). Figure 2.10 (2019) also shows that treatments started to differentiate since initiation of variable rate irrigation (July 12th, 2019). Stomatal conductance of treatments that received less or no water were generally lower than fully irrigated treatment. As found in Nemeskéri et al. (2015), plants tend to close stomata to save water when experiencing water stress and therefore lower SC. One of the reasons for that is the direct correlation that SC has with ET_c (Sharkey and Seemann, 1989).

In 2019, the difference in SC values between treatment 0% to treatment 100% was larger during the last two dates, August 6th (629 mmol/m^{2}s) and August 9th (717 mmol/m^{2}s), respectively, due to the difference in irrigation treatments. In addition, similar results were reported by Chibarabada et al. (2019) for a study in South Africa with bambara groundnut (*Vigna subterranea* L.), dry bean (Phaseolus vulgaris L.) and groundnut (*Arachis hypogaea* L.), which reported differences of more than 300 mmol m^{-2} s^{-1} between full irrigated treatment (680 mmol m^{-2} s^{-1}) and rainfed treatment (310 mmol m^{-2} s^{-1}).

2.3.3 Leaf Area Index

Figure 2.11 shows LAI values of different irrigation treatments on different dates in 2019. As shown in Figure 2.11, LAI average values for each treatment were

significantly different (*p-value* = 0.04) among irrigation treatments. Plots that received higher amount of water presented higher LAI values, especially towards the end of the growing season. The readings presented in Figure 2.11 were taken before the pod-filling stage due to the hailstorm that took place in the area on August 14th. In a scenario without a hailstorm and LAI being continuously measured until the end of the season, we would expect LAI values to decrease after the plant reached maturity at about 60 days after planting (Medeiros et al., 2001; Meireles et al., 2002).

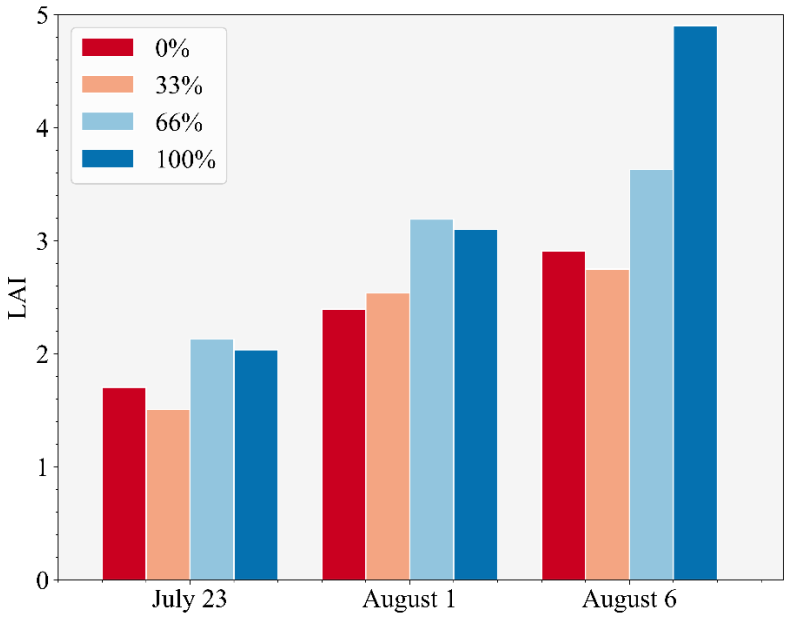

Figure 2.11. Leaf area index (LAI) for different irrigation treatments in 2019 growing season. Different colors represent different irrigation treatments. Readings were taken before the hailstorm (August 14th).

2.3.4 CWSI Baselines

Figure 2.12 depicts the crop water stress index average baselines (lower and upper baselines) found in this study and Table 2.1 depicts the formula for the individual lower and upper baselines calculated for each year and the formula for the average baselines. For

the upper baseline, because 2018 and 2019 were wetter than normal years, only data from dry period of the season was used, which explains only having three data points for determination of upper baseline in 2018.

Table 2.1. Lower baseline, upper baseline and parameters found for seasons 2018, 2019 and the average for the two seasons.

	Lower baseline	R^2	n[a]	Upper baseline	n[b]	SD[c]
2018	Tc – Ta = 2.67 - 1.57 VPD	0.80	16	3.77	3	0.83
2019	Tc – Ta = 2.83 - 1.56 VPD	0.79	9	3.76	8	0.24
Avg.	Tc – Ta = 2.78 - 1.59 VPD	0.81	25	3.76	11	0.42

Note: [a]n represents the number of measurements used to calculate lower baseline.
[b]n represents the number of measurements used to calculate upper baseline.
[c]SD represents standard deviation of values used to calculate upper baseline.

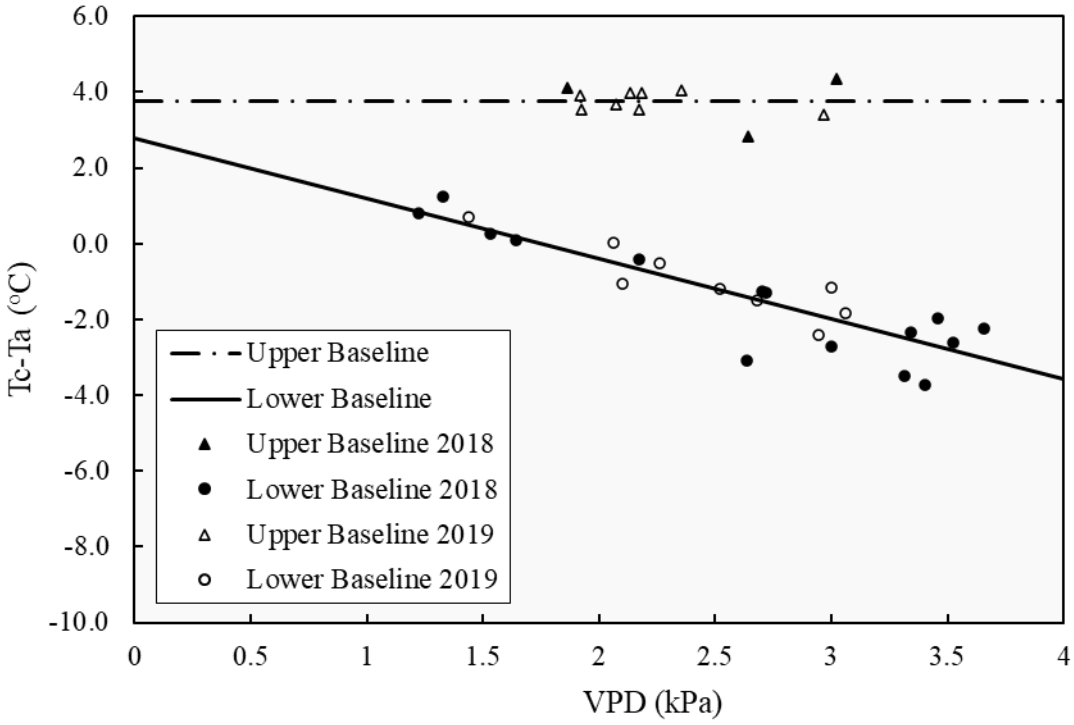

Figure 2.12. Average lower and upper baseline developed in this study for dry edible beans and observation points for 2018 and 2019 in Scottsbluff, Nebraska.

In 2018, data from all plots from 0% treatment were used to calculate the upper baseline and all plots from 100% treatment were used to calculate the lower baseline. In 2019, to calculate the upper baseline, a subset of data from 0% treatment was used because the southern plots were flooded during part of the season. Lower baseline was calculated using all data from plots of 100% treatment. Figure 2.13 shows soil volumetric water content (VWC) of plots in 2019 from 0% treatment (first row) and 100% treatment (second row) located in the different blocks. Four different depths are represented in the graphs (30, 60, 90, and 120 cm). The first row of Figure 2.13 (0% treatment) shows that VWC of plots at block one (North Block) at 30 cm and 60 cm depths were close to permanent wilting point of the soil at study area (10%). However, this is not true for plots of 0% treatment located at either middle or south blocks. A digital elevation model (DEM) map of the area is shown in Figure 2.14. In the map, it is seen that the north part of the field has a higher elevation than the south part.

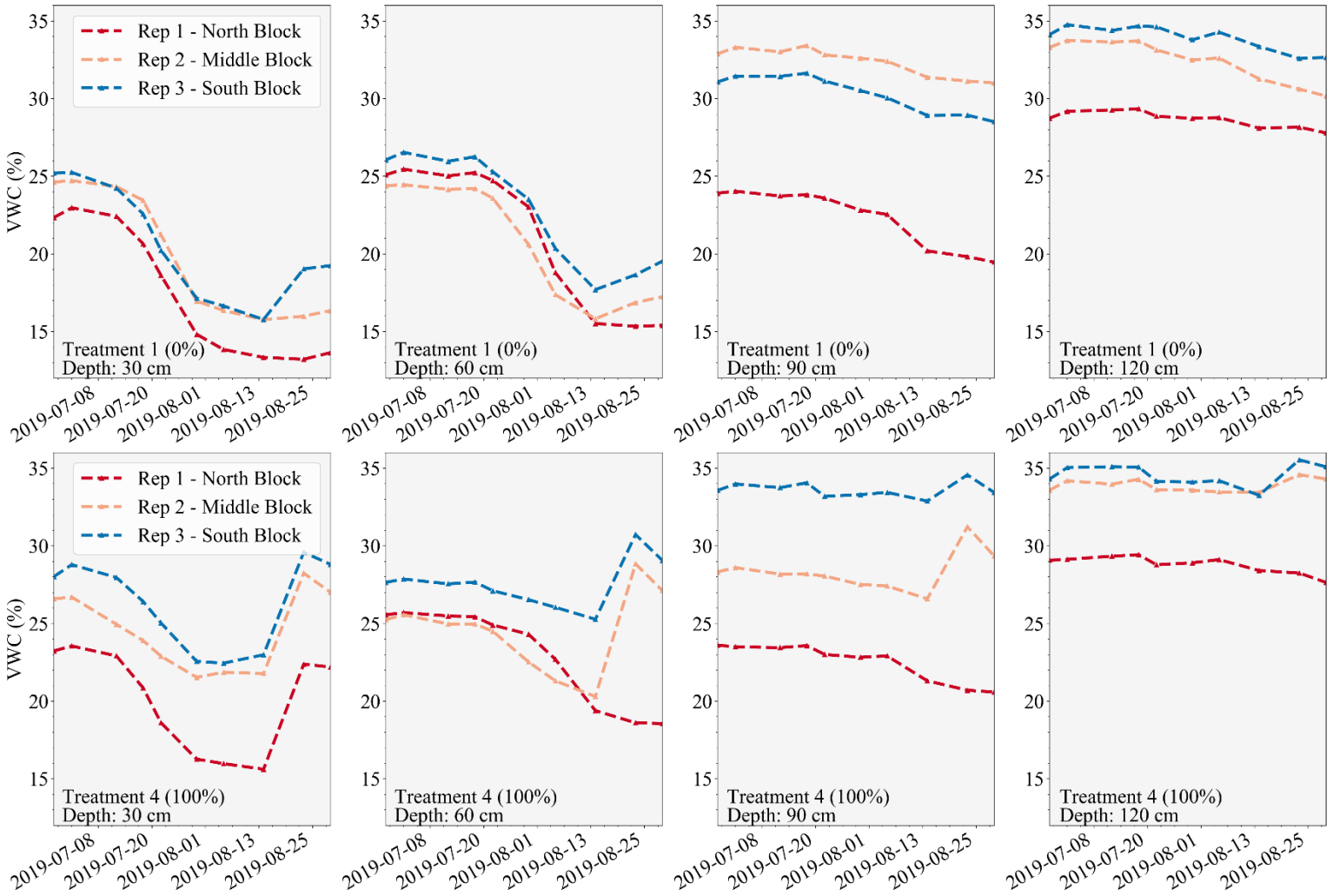

Figure 2.13. Volumetric water content (VWC, %) for treatment 0% (upper row) and treatment 100% (lower row) of different depths at the 3 blocks (north, middle, south) due to slope of experimental field.

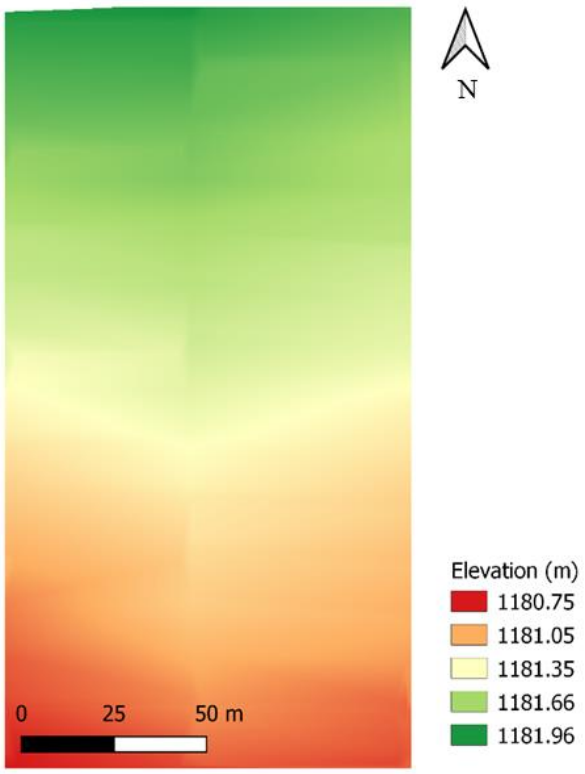

Figure 2.14. Digital elevation model (DEM) map of study area in Scottsbluff, NE.

Figure 2.15 shows lower baselines found in this study and by other researchers for common beans. Figure 2.15 shows that lower baselines have different slopes and intercepts depending on the location where the study took place, despite the fact that all locations are semi-arid climate. This result reinforces the importance of calculating localized baselines when using CWSI.

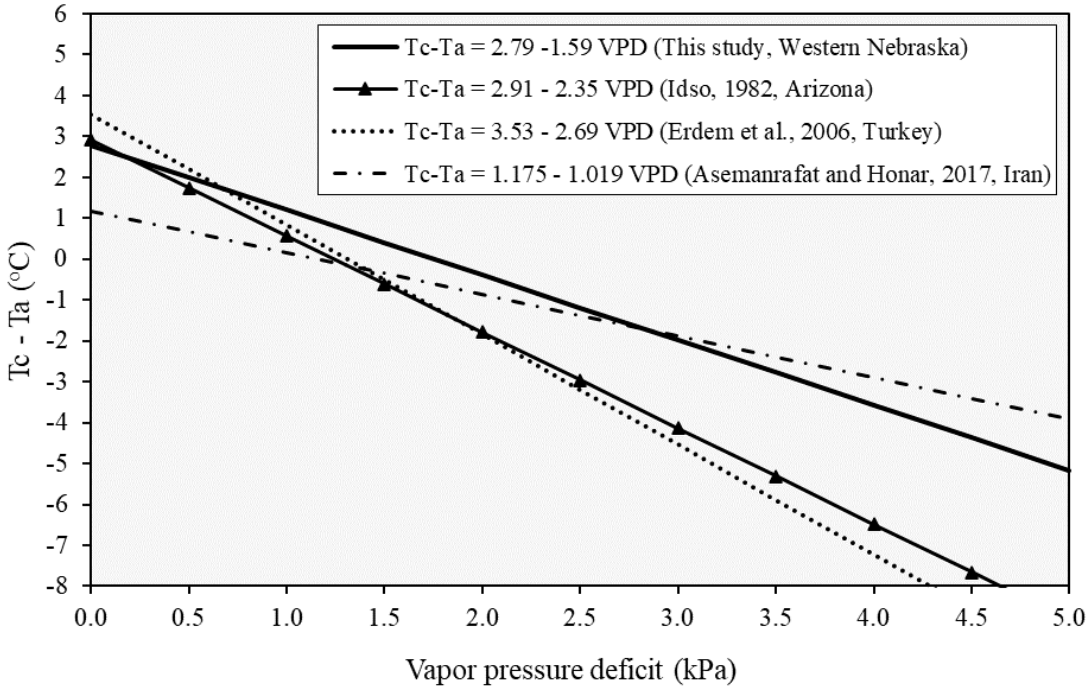

Figure 2.15. Comparison of lower baselines from this study with other studies with common beans.

2.3.5 CWSI calculation for different irrigation treatments

As mentioned previously, canopy temperature is the cornerstone in CWSI calculation. Figure 2.16 and Figure 2.17 show DEB canopy temperature (°C) for the four irrigation treatments along 2018 and 2019 season, respectively. Difference in canopy temperature can be seen especially during the day among the different irrigation treatments. Zoomed in versions of differences in canopy temperature among different treatments during three consecutive days are shown in Figure 2.18 and Figure 2.19 for 2018 and 2019 growing seasons, respectively.

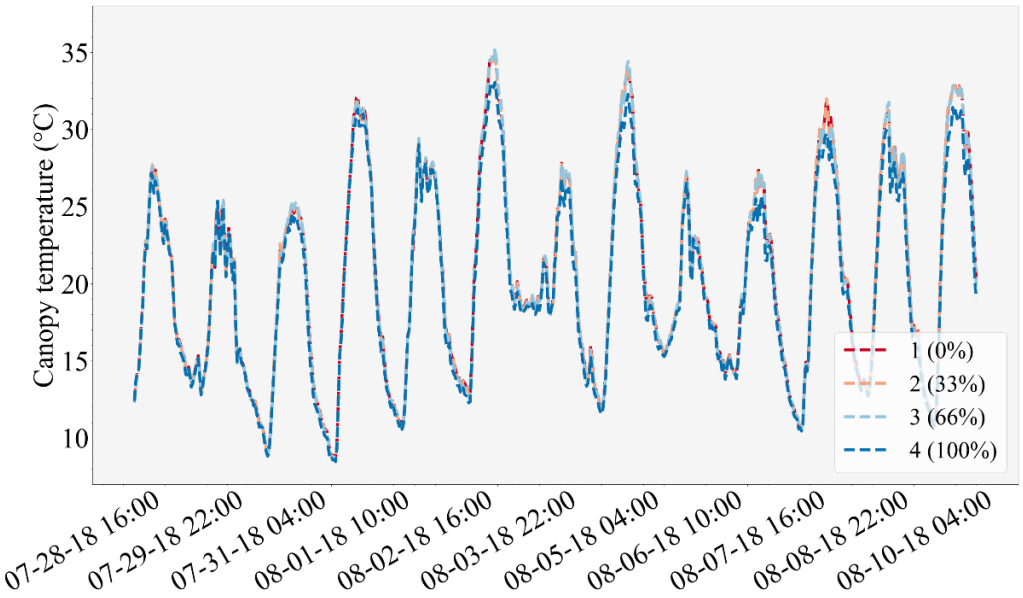

Figure 2.16. Dry edible bean canopy temperature for different treatments along 2018 season.

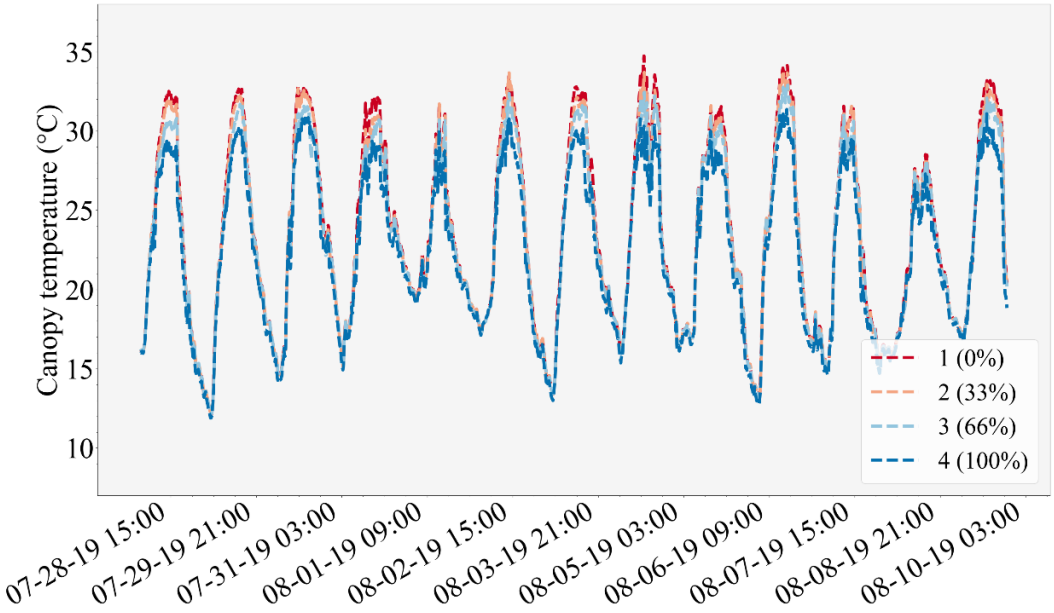

Figure 2.17. Dry edible bean canopy temperature for different treatments along 2019 season.

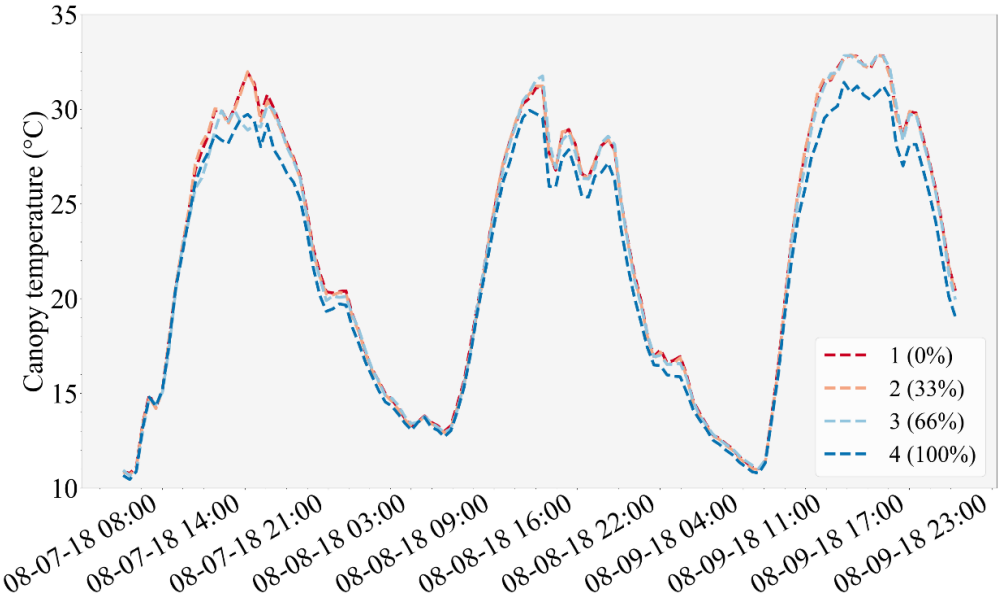

Figure 2.18. Dry edible bean canopy temperature for different irrigation treatment for 3 consecutive days during 2018 season.

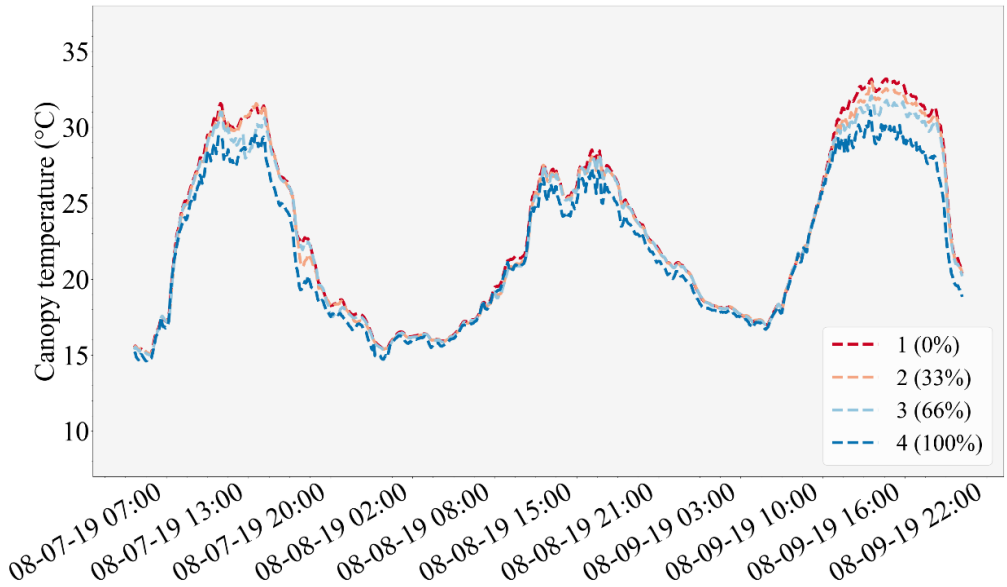

Figure 2.19. Dry edible bean canopy temperature for different irrigation treatment for 3 consecutive days during 2019 season.

Figure 2.20 and Figure 2.21 show calculated CWSI values for the four treatments along the growing seasons in 2018 and 2019, respectively. CWSI values from all

treatments show diurnal pattern (Figure 2.20 and Figure 2.21). Some extreme values are also observed along the season, and there are several possible factors that could explain the extreme values. Values vary from -5.16 to 2.95 in 2018 and from -5.33 to 2.55 in 2019. In this study, it was observed that the extreme values occurred mainly when the difference between canopy and air temperature was greater than ± 3^{o}C, which led to high CWSI values (~ 3) if the difference was positive, and low CWSI values (~ -5) if the difference was negative. High winds could be a possible explanation for extremely high CWSI values, which are both mainly observed in the afternoons. Since DEB plants are short and canopy cover was not at 100%, high winds would cause the plants to move and IRT could record temperature from soil instead of canopy. In 2019, the highest CWSI value of 2.54 was observed on a windy day (August 4th – flowering growth stage) with winds speeds around 6 m/s measured at 3 m. A possible explanation for extreme low CWSI values is the low nighttime air temperatures observed in the summers in western Nebraska. One of the examples observed was CWSI value of -5.02 which occurred in an early morning (August 3rd, 2019 at 6:00 am) after a cold night (average night air temperature of 15.4 ^{o}C). Those two assumptions are in agreement to results presented by Gardner et al. (1992a), who mention that some of the factors that lead to values out of the range of zero and one are dense clouds, high wind speeds and lower observed air temperatures than temperature used to create baselines. Figure 2.22 and Figure 2.23 are "zoomed in" version of previous graphs, which shows three consecutive days when beans were during maximum canopy cover in 2018 and 2019 growing seasons, respectively.

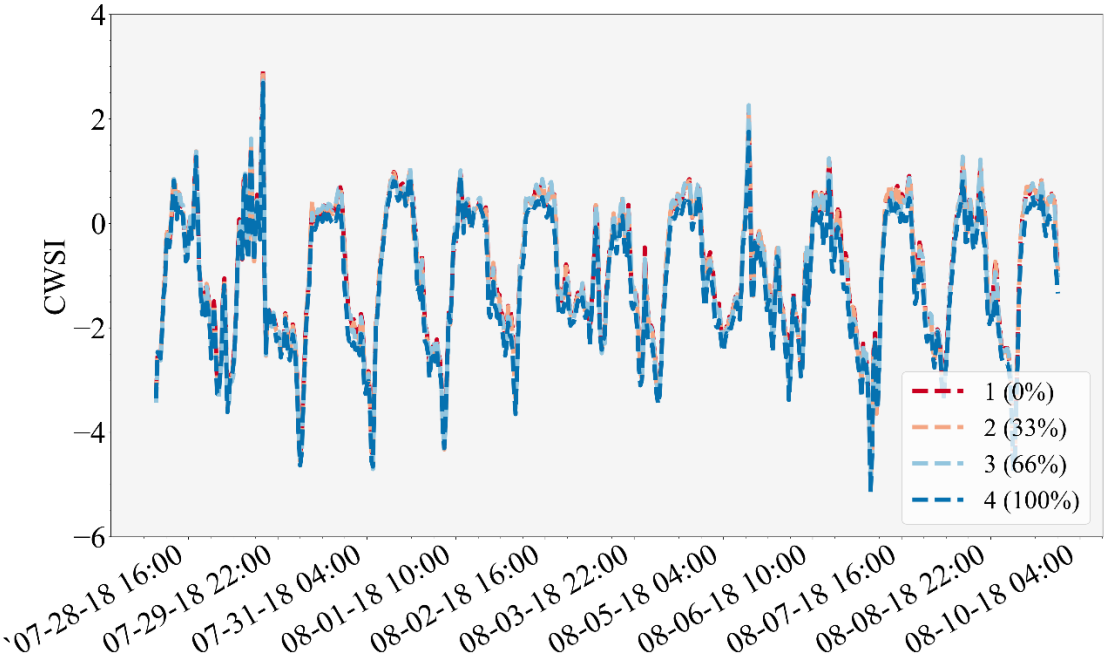

Figure 2.20. Crop water stress index (CWSI) values for dry edible bean planted in Scottsbluff, Nebraska for four treatments (0%, 33%, 66%, and 100%) along the 2018 season.

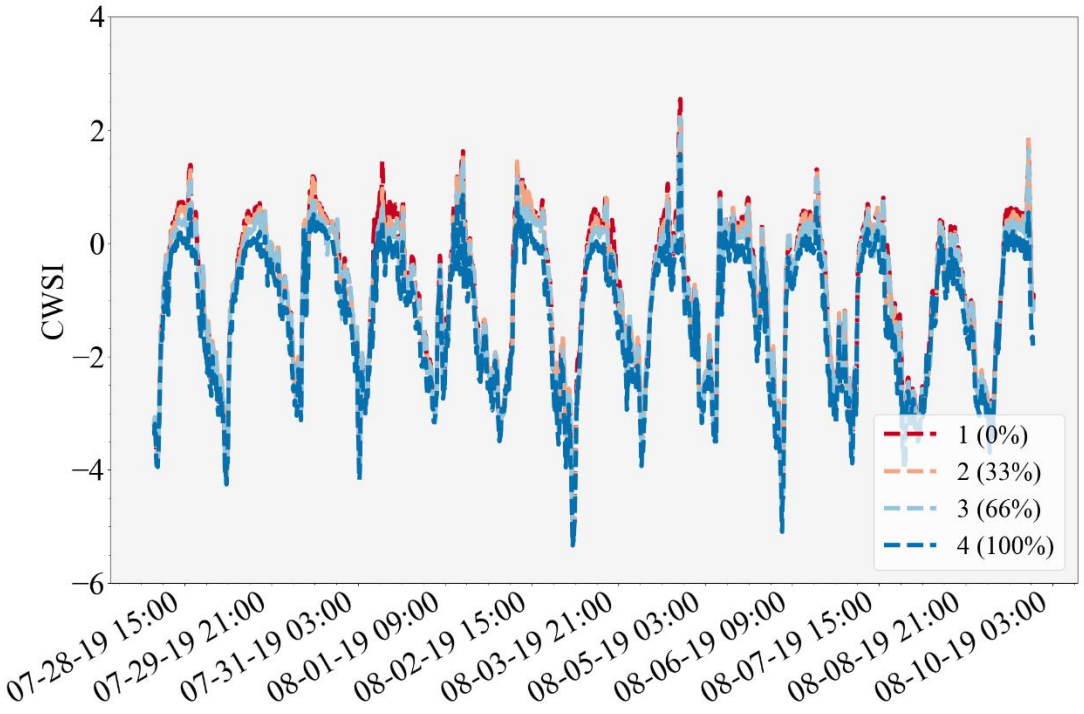

Figure 2.21. Crop water stress index (CWSI) values for dry edible bean planted in Scottsbluff, Nebraska for four treatments (0%, 33%, 66%, and 100%) along the 2019 season.

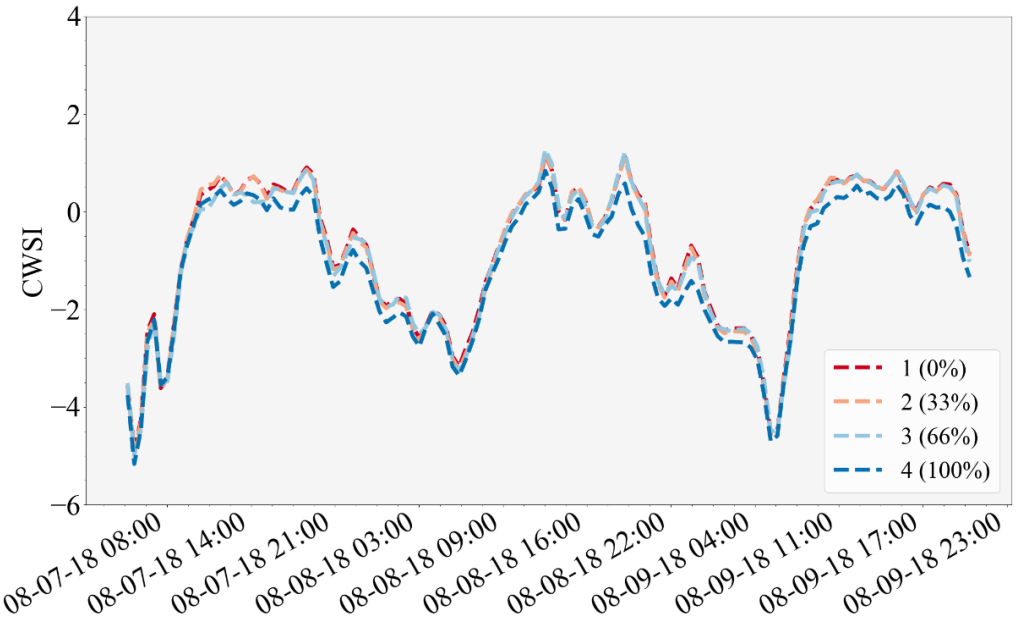

Figure 2.22. Crop water stress index (CWSI) values for three days for dry edible bean planted in Scottsbluff, Nebraska for four treatments (0%, 33%, 66%, and 100%) along the 2018 season.

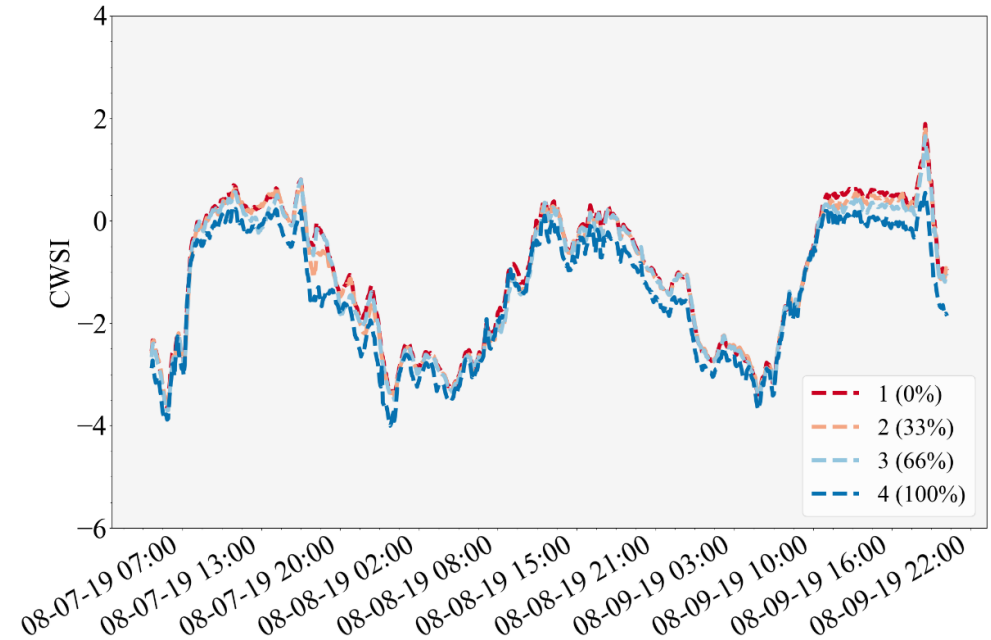

Figure 2.23. Crop water stress index (CWSI) values for three days for dry edible bean planted in Scottsbluff, Nebraska for four treatments (0%, 33%, 66%, and 100%) along the 2019 season.

When selecting only data collected between 12:00 PM to 3:00 PM, the range in CWSI values were smaller than when using data collected during the entire day. CWSI varied from -1.13 to 0.79 for 0% treatment and from -1.22 to 0.64 for 100% treatment in 2018 (Figure 2.24); in 2019 CWSI varied from -0.02 to 0.84 for 0% treatment and from -0.40 to 0.30 for 100% treatment (Figure 2.25). During that period (12:00 PM and 3:00 PM), CWSI values were significantly different among treatments by having p-values of 0.0143 (2018) and 4.2×10^{-6} (2019). In 2018, CWSI of treatment three (66%) and treatment four (100%) were significantly smaller than CWSI of treatment one (0%), with p-values of 0.040 and 0.025, respectively. For 2019, CWSI of treatment three (66%) and treatment four (100%) were significantly smaller than treatment one (0%) and treatment two (33%). When comparing treatments three (66%) and four (100%) with treatment one (0%), p-values were 2.6×10^{-5} and 1.8×10^{-4}, respectively. When comparing treatments three (66%) and four (100%) with treatment two (33%), p-values were 0.02 and 0.05, respectively.

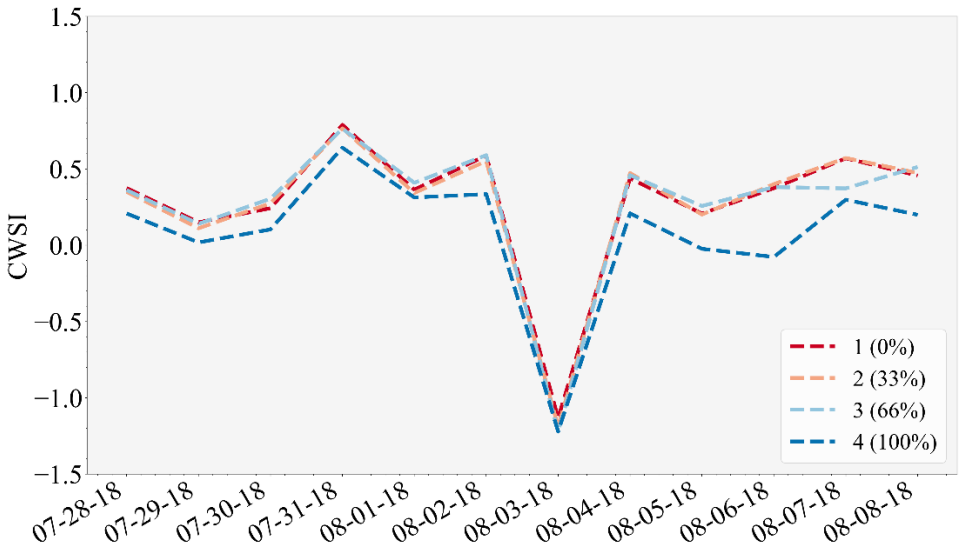

Figure 2.24. CWSI values between 12:00 pm and 3:00 pm for four treatments in 2018.

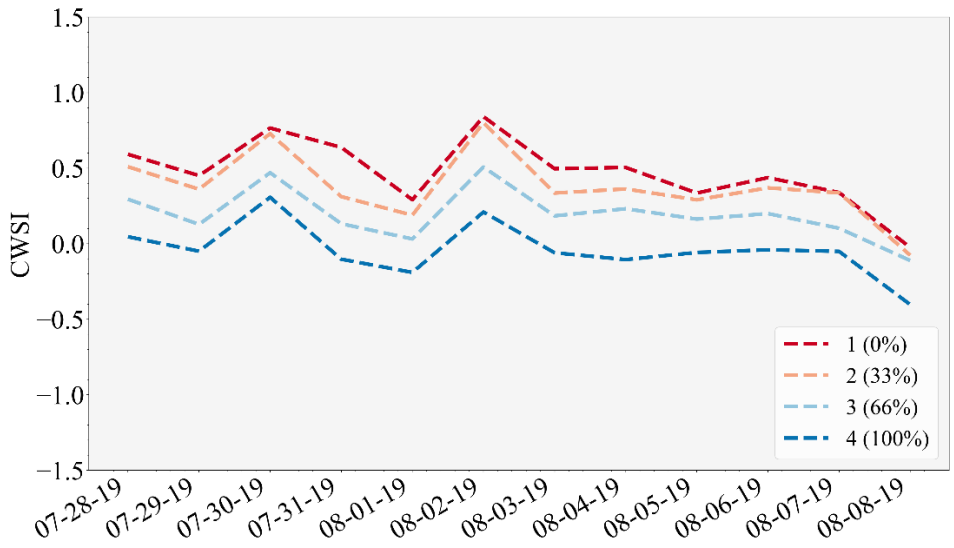

Figure 2.25. CWSI values between 12:00 pm and 3:00 pm for four treatments in 2019.

2.3.6 Sensitivity analysis on CWSI calculation

A sensitivity analysis was conducted to determine how variation of upper baseline, intercept and slope of lower baseline can affect CWSI calculation. Sensitivity analyses were conducted using data from all treatments from 2018 and 2019. Upper baseline values were varied from 2.96 to 4.56 at 0.2 ºC increments. Figure 2.26 and Figure 2.27 depict the variation in CWSI values when changing upper baseline values for 2018 and 2019, respectively. It is observed that in both years, variation in mean and range of CWSI values for all treatments was minimal when upper baseline value was changed.

Figure 2.28 and Figure 2.29 show the variation in CWSI values of all treatments when lower baseline intercept value was varied for 2018 and 2019, respectively. In both years, it is observed that as intercept increases, mean CWSI decreases while range of CWSI increases, although those variations were trivial.

As slope of lower baseline is changed, Figure 2.30 and Figure 2.31 depict the variation in CWSI values for 2018 and 2019, respectively. The variation in mean CWSI and range of CWSI is mostly observed for data of treatment four (100%). By changing slope from -0.79 to -2.39, mean CWSI of treatment four (100%) changes from -0.31 to 0.40 for 2018 and from -0.69 to 0.26 for 2019. As the slope becomes less negative, mean CWSI values start to decrease and standard deviation of CWSI values becomes larger. The opposite is true when slope values become more negative: mean CWSI values start to increase and standard deviation in CWSI values becomes smaller.

Comparing the change in CWSI values caused by the variation in the three parameters, slope of the lower baseline was the parameter that presented the biggest change of CWSI in terms of mean and range of values, as seen in Figures 2.32 and 2.33, which depict the change in CWSI values when varying the slope and the intercept of lower baseline and upper baseline values for treatment four (100%) for 2018 and 2019, respectively. The baseline scenarios for that analysis, represented as 0.0 in the x-axis in Figure 2.32 and Figure 2.33, are the parameters found for in this study (slope = -1.59, intercept = 2.78, and upper baseline = 3.76). The sensitivity analysis using 100% treatment data shows that the lower baseline slope has the biggest impact in CWSI value and the upper baseline the least impact. The same is observed for data from treatment one (0%), as shown in Figure 2.34 and Figure 2.35.

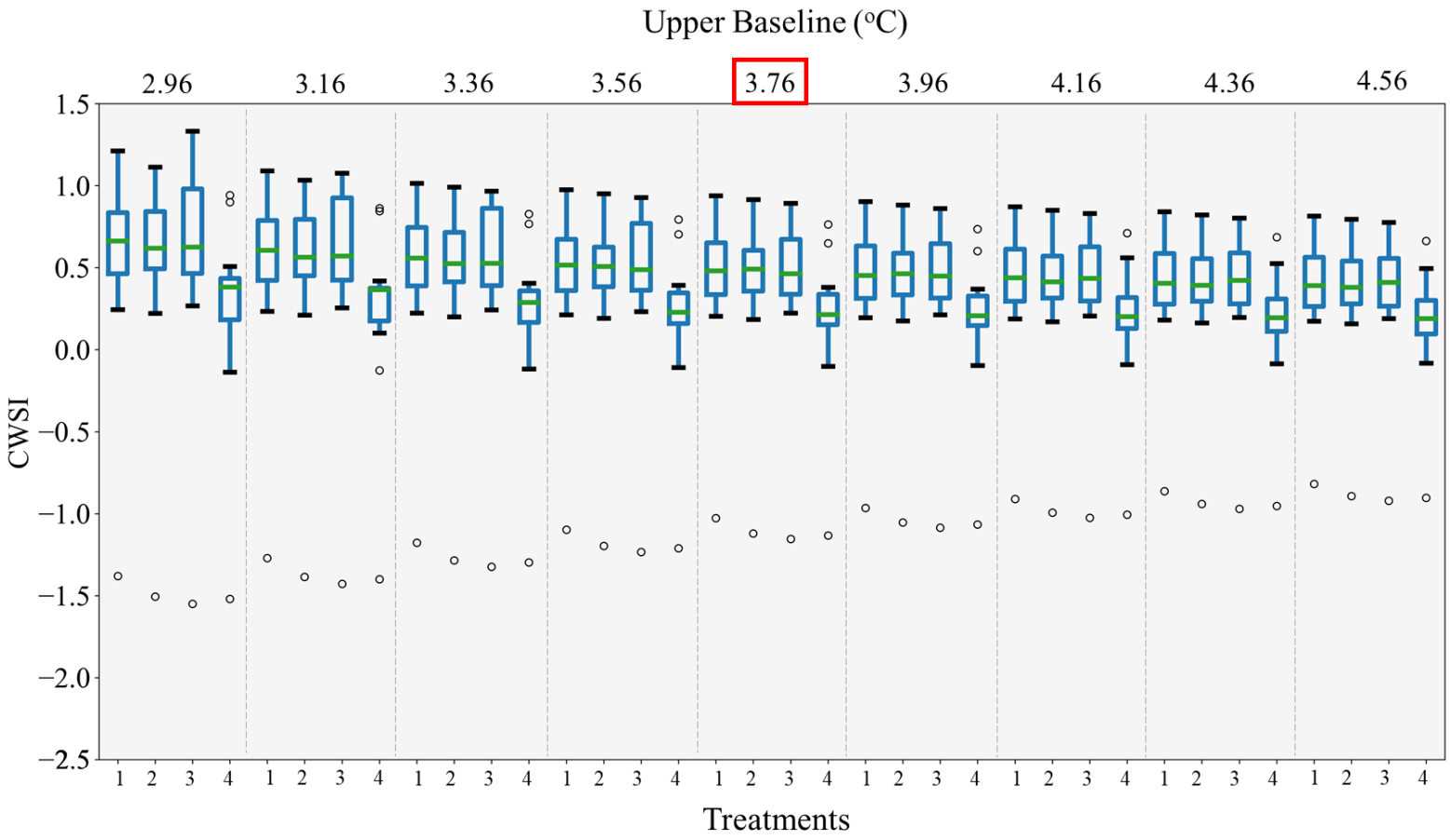

Figure 2.26. CWSI variation with changing in upper baseline value for all treatments (treatment 1 - 0%, treatment 2 - 33%, treatment 3 - 66% and treatment 4 - 100%) for 2018. Red square shows average upper baseline value found for this study.

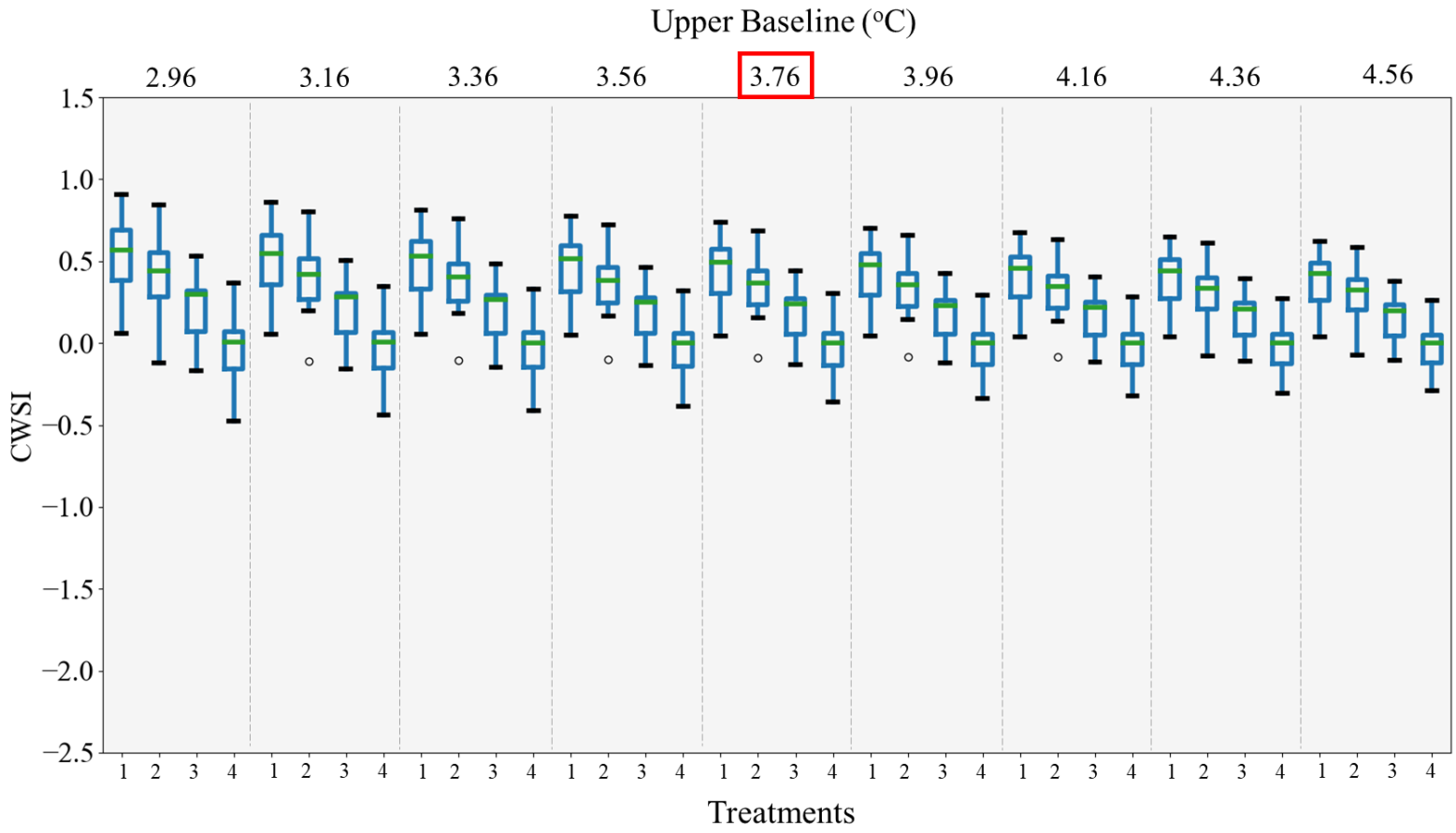

Figure 2.27. CWSI variation with changing in upper baseline value for all treatments (treatment 1 - 0%, treatment 2 - 33%, treatment 3 - 66% and treatment 4 - 100%) for 2019. Red square shows average upper baseline value found for this study.

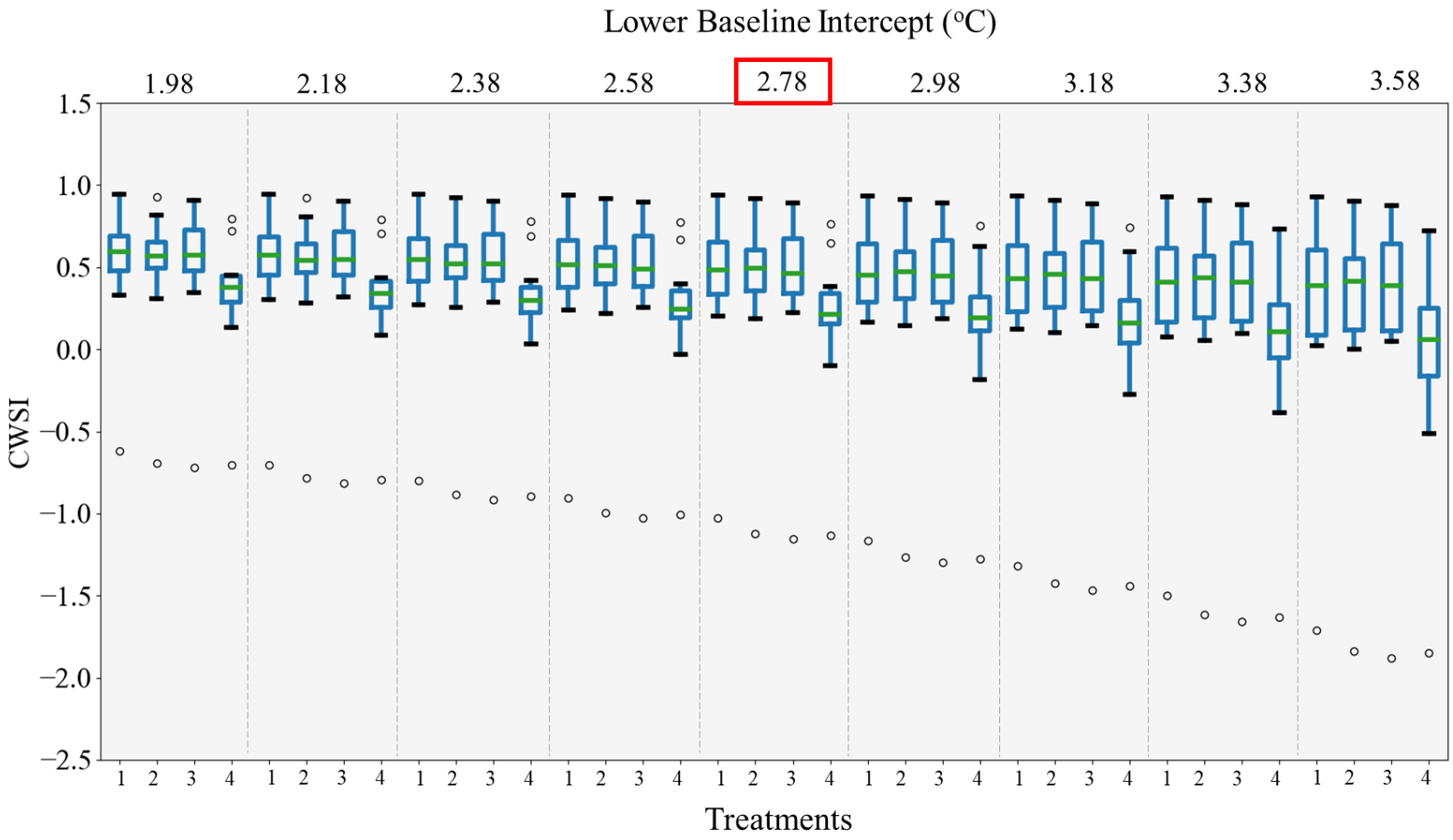

Figure 2.28. CWSI variation with changing in lower baseline intercept value for all treatments (treatment 1 - 0%, treatment 2 - 33%, treatment 3 - 66% and treatment 4 - 100%) for 2018. Red square shows average lower baseline intercept value found for this study.

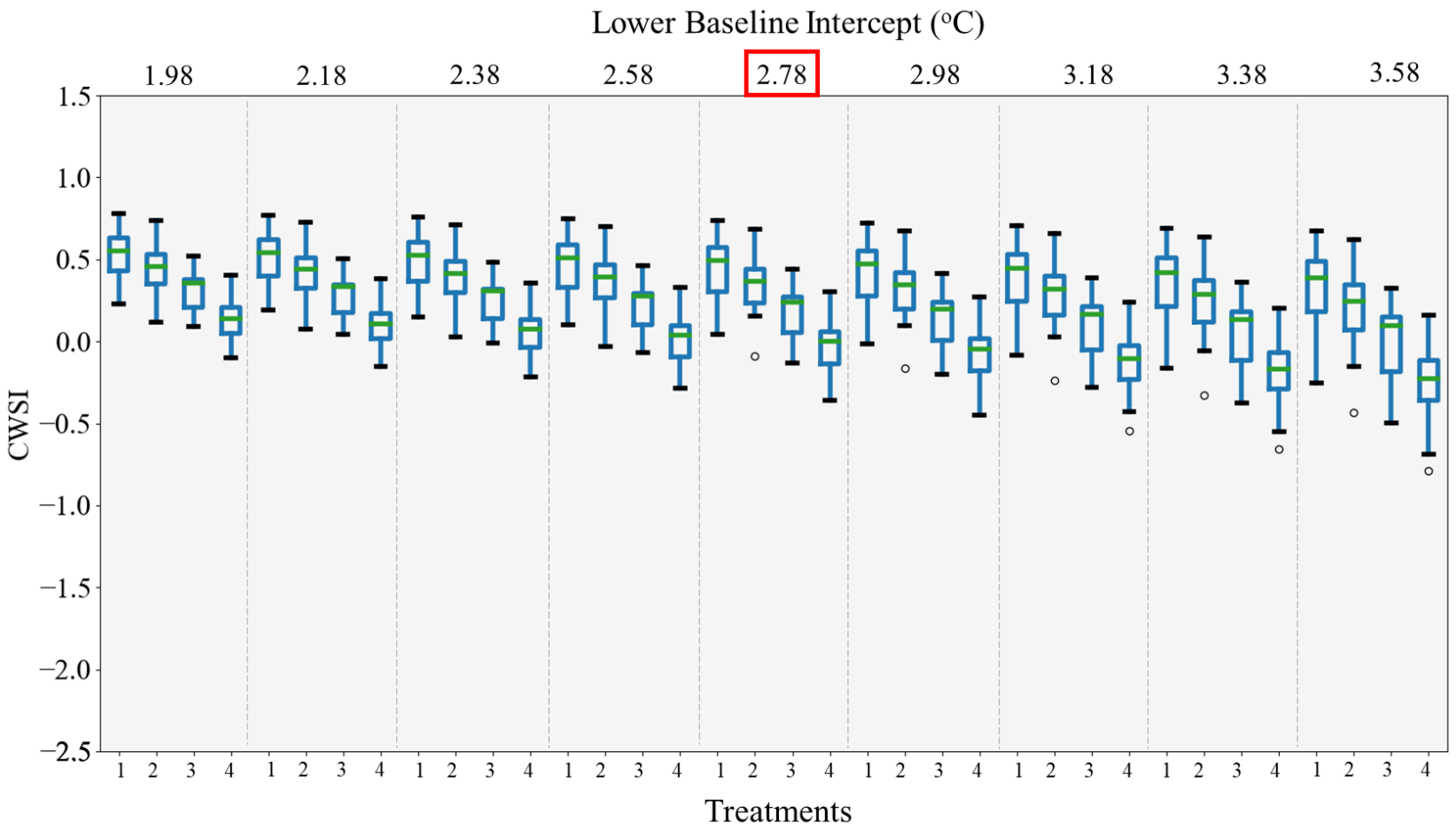

Figure 2.29. CWSI variation with changing in lower baseline intercept value for all treatments (treatment 1 - 0%, treatment 2 - 33%, treatment 3 - 66% and treatment 4 - 100%) for 2019. Red square shows average lower baseline intercept value found for this study.

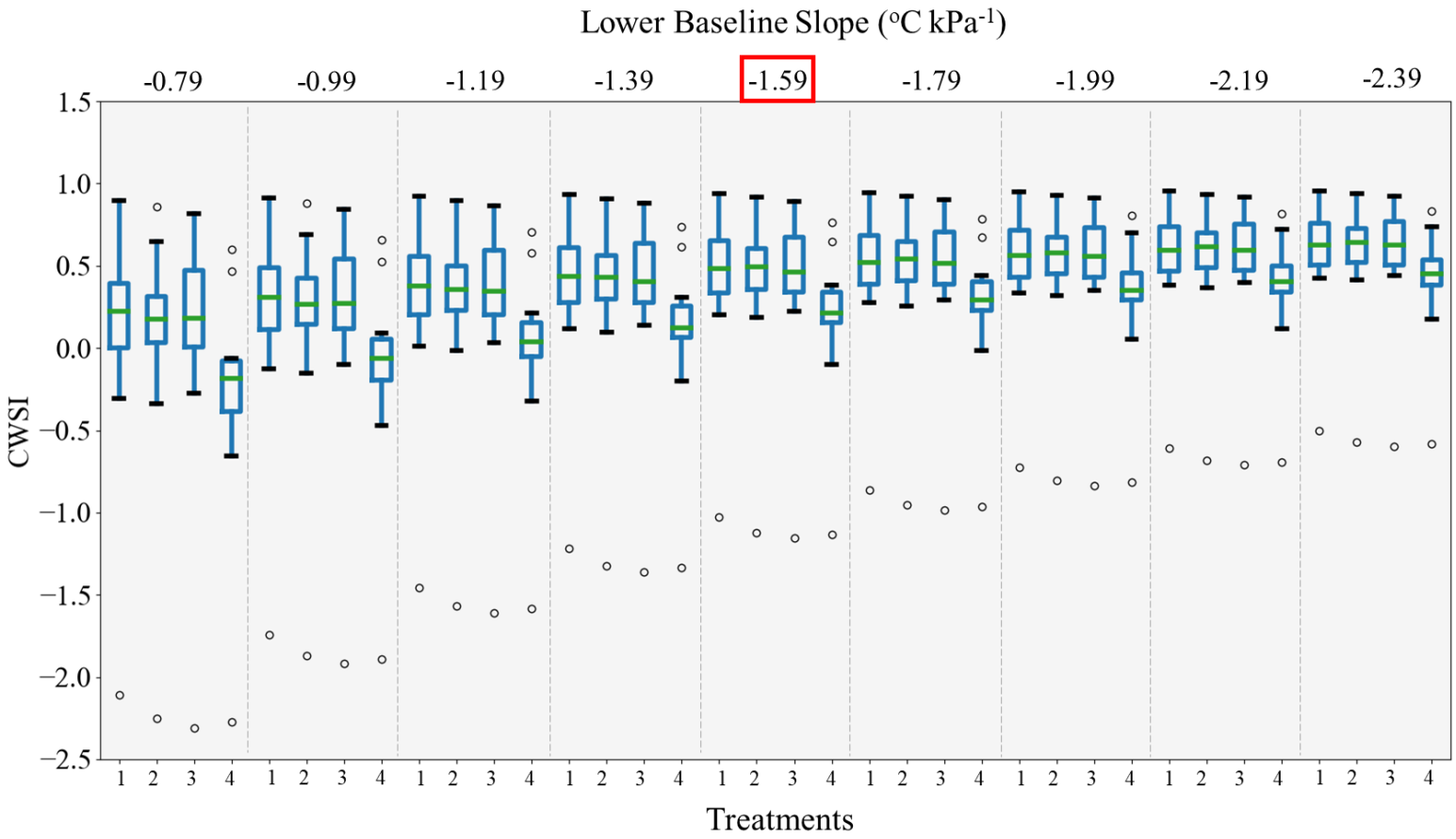

Figure 2.30. CWSI variation with changing in lower baseline slope value for all treatments (treatment 1 - 0%, treatment 2 - 33%, treatment 3 - 66% and treatment 4 - 100%) for 2018. Red square shows average lower baseline slope value found for this study.

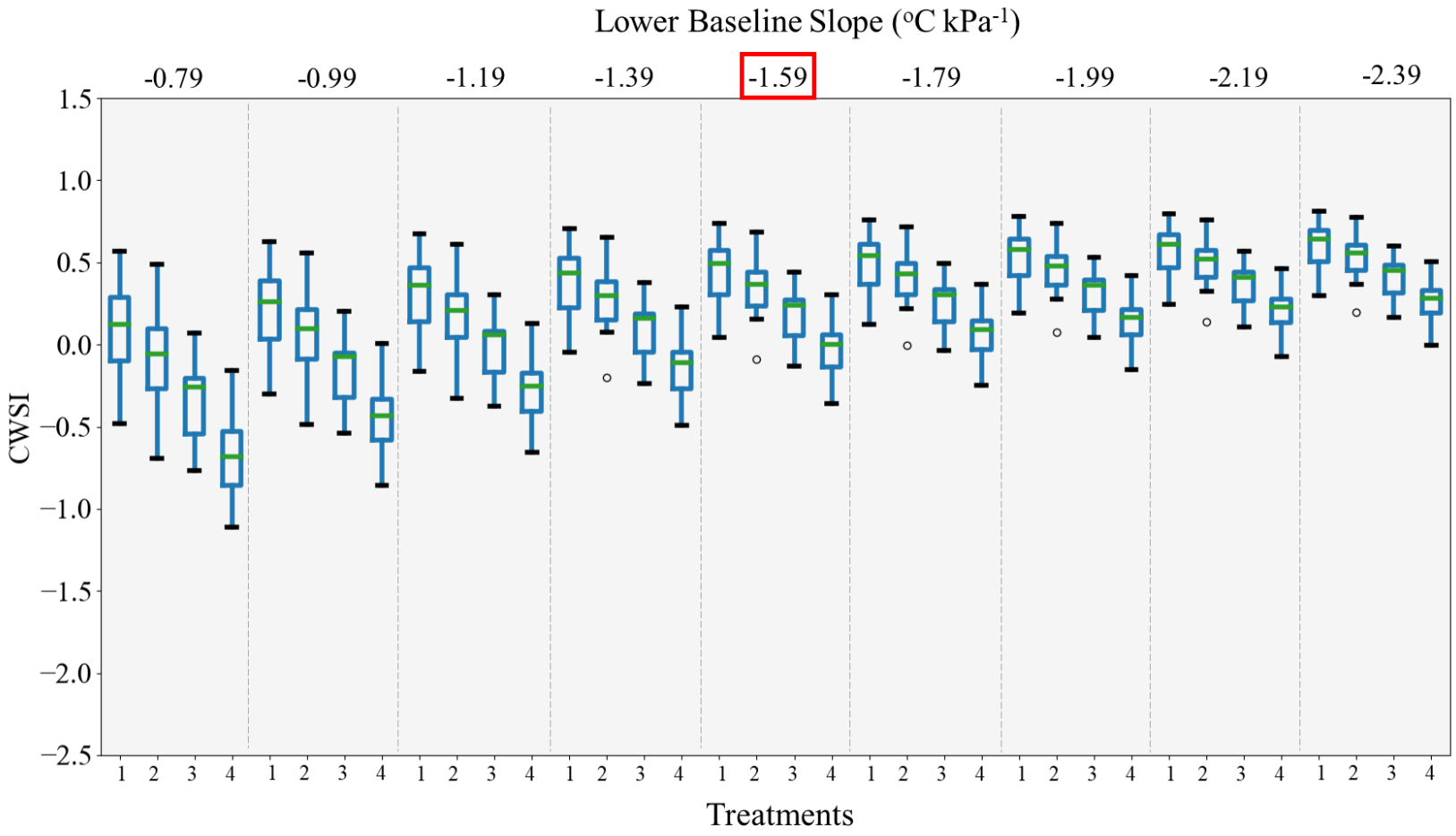

Figure 2.31. CWSI variation with changing in lower baseline slope value for all treatments (treatment 1 - 0%, treatment 2 - 33%, treatment 3 - 66% and treatment 4 - 100%) for 2019. Red square shows average lower baseline slope value found for this study.

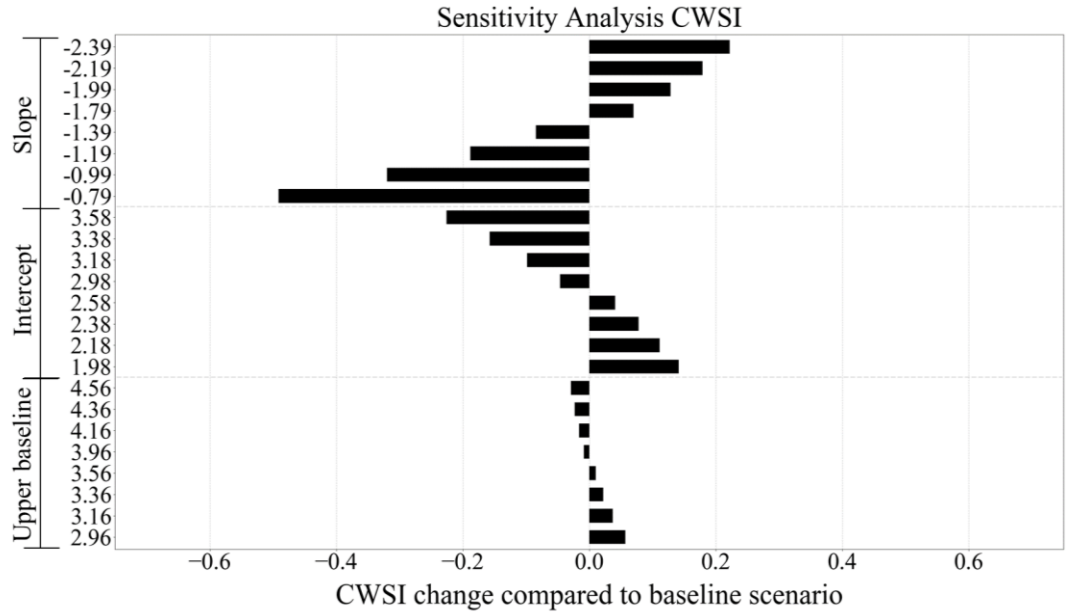

Figure 2.32. CWSI change by variating lower baseline slope and intercept and upper baseline values for 100% treatment data from 2018. Variation is represented in comparison with the baseline scenario, which are the parameters values found in this study (slope = -1.59, intercept = 2.78, and upper baseline = 3.76).

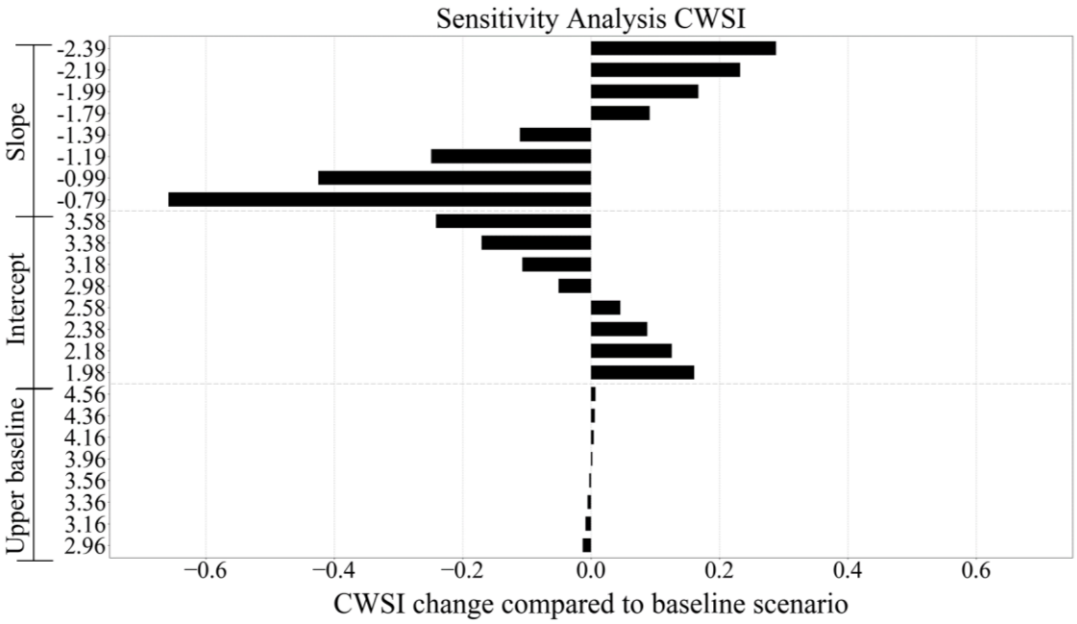

Figure 2.33. CWSI change by variating lower baseline slope and intercept and upper baseline values for 100% treatment data from 2019. Variation is represented in comparison with the baseline scenario, which are the parameters values found in this study (slope = -1.59, intercept = 2.78, and upper baseline = 3.76).

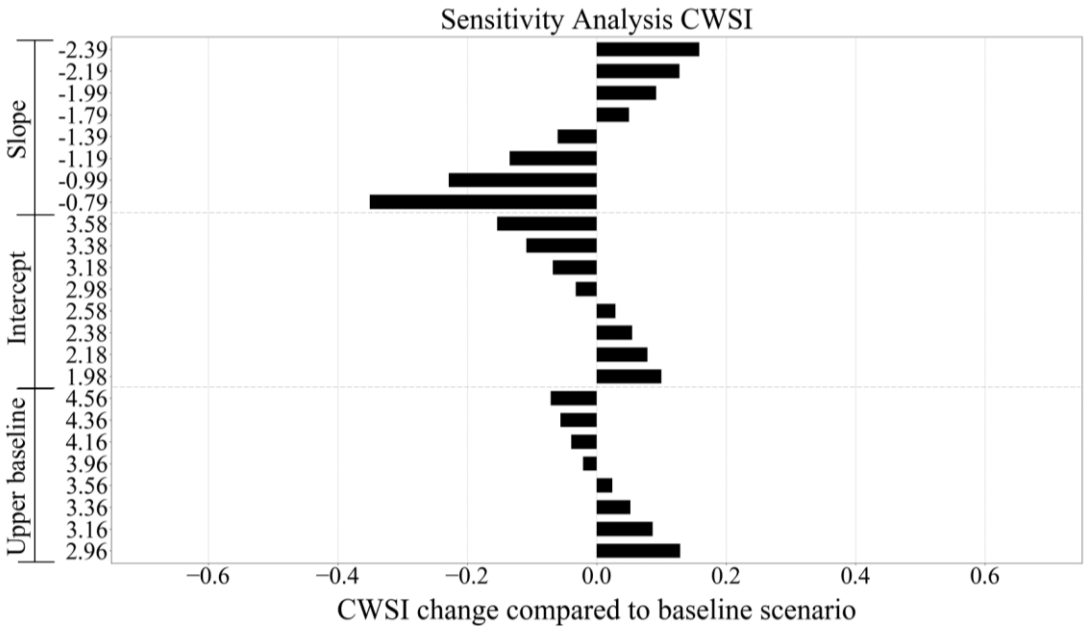

Figure 2.34. CWSI change by variating lower baseline slope and intercept and upper baseline values for 0% treatment data from 2018. Variation is represented in comparison with the baseline scenario, which are the parameters values found in this study (slope = -1.59, intercept = 2.78, and upper baseline = 3.76).

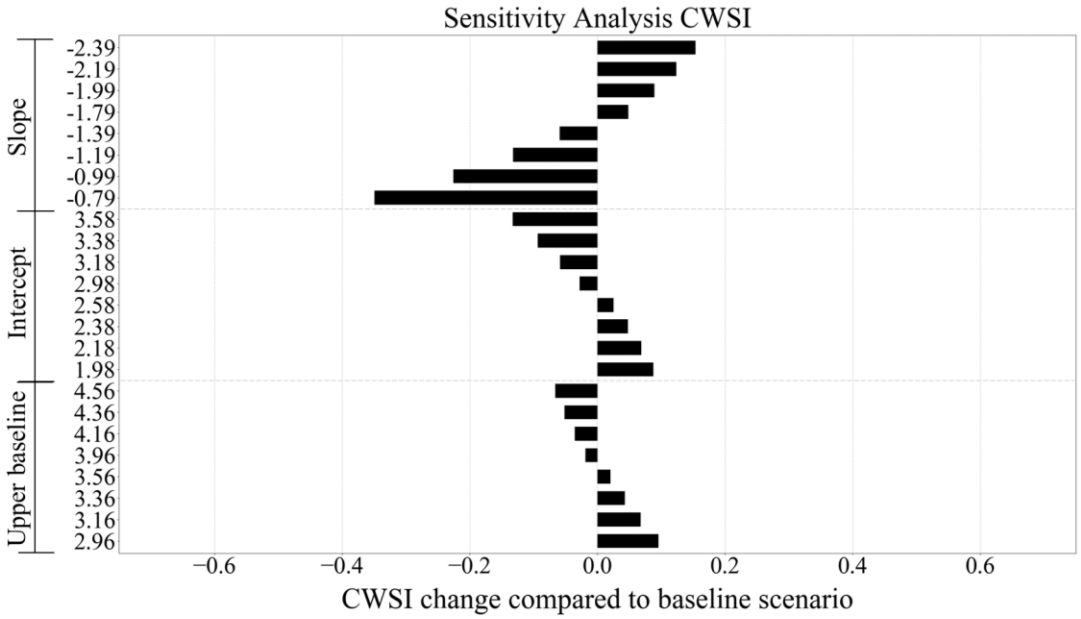

Figure 2.35. CWSI change by variating lower baseline slope and intercept and upper baseline values for 0% treatment data from 2019. Variation is represented in comparison with the baseline scenario, which are the parameters values found in this study (slope = -1.59, intercept = 2.78, and upper baseline = 3.76).

2.4 Conclusion

This study had two main objectives. The first objective of this study was to develop CWSI lower and upper baselines for DEB in western Nebraska. Baselines calculated for both seasons (2018 and 2019) were similar. For the lower baseline, the following equations were found: Tc – Ta = 2.67 - 1.57 VPD (2018), and Tc – Ta = 2.83 - 1.56 VPD (2019). For the upper baseline, values of 3.77 and 3.76 were found in 2018 and 2019 growing seasons, respectively. The average lower baseline was Tc – Ta = 2.78 - 1.59 VPD (n = 25, R2 = 0.81) and upper baseline was Tc – Ta = 3.76 (n = 11, SD = 0.42). Also, to analyze which component of CWSI calculation (upper baseline, intercept and slope of lower baseline) mostly contributed to CWSI variations, sensitivity analyses were performed. Results showed that slope of lower baseline had the biggest effect on CWSI calculation.

The second objective of this study was to evaluate the response of CWSI for DEB at four irrigation treatments that ranged from dryland (0%) to fully irrigated treatment (100%). CWSI was able to capture difference in plant water stress of the four irrigation treatments. This difference was mostly apparent between 12:00 and 3:00 PM.

REFERENCES

Al-Ghobari, H. M., Dewidar, A. Z. (2018). Integrating deficit irrigation into surface and subsurface drip irrigation as a strategy to save water in arid regions. *Agricultural Water Management*, *209*, 55–61.

Allen, R. G., Pereira, L. S., Raes, D., Smith, M. (1998). Crop evapotranspiration-Guidelines for computing crop water requirements-FAO Irrigation and drainage paper 56. *Fao*, *Rome*, *300*(9), D05109.

Andales, A. A., Chávez, J. L. (2011). ET-Based Irrigation Scheduling, 39–46.

Asemanrafat, M., Honar, T. (2017). Effect of water stress and plant density on canopy temperature, yield components and protein concentration of red bean (Phaseolus vulgaris L. cv. Akhtar). *International Journal of Plant Production*, *11*(2).

Bos, M. (1980). Irrigation efficiencies at crop production level.

Bourgault, M., Madramootoo, C. A., Webber, H. A., Dutilleul, P., Stulina, G., Horst, M. G., Smith, D. L. (2013). Legume Production and Irrigation Strategies in the A ral Sea Basin: Yield, Yield Components, Water Relations and Crop Development of Common Bean (P haseolus vulgaris L.) and Mungbean (V igna radiata (L.) W ilczek). *Journal of Agronomy and Crop Science*, *199*(4), 241–252.

Calvache, M., Reichardt, K., Bacchi, O. O. S., Dourado-Neto, D. (1997). Deficit irrigation at different growth stages of the common bean (Phaseolus vulgaris L., cv. Imbabello). *Scientia Agricola*, *54*(SPE), 1–16.

Chibarabada, T. P., Modi, A. T., Mabhaudhi, T. (2019). Water use of selected grain

legumes in response to varying irrigation regimes. *Water SA*, *45*(1), 110–120.

Comas, L. H., Trout, T. J., DeJonge, K. C., Zhang, H., Gleason, S. M. (2019). Water productivity under strategic growth stage-based deficit irrigation in maize. *Agricultural Water Management*, *212*, 433–440.

da Silva, B. B., Rao, T. V. R. (2005). The CWSI variations of a cotton crop in a semi-arid region of Northeast Brazil. *Journal of Arid Environments*, *62*(4), 649–659.

Decagon Device Inc. (2016). *Leaf Porometer Operator's Manual*. Retrieved from www.decagon.com

DeJonge, K. C., Taghvaeian, S., Trout, T. J., Comas, L. H. (2015). Comparison of canopy temperature-based water stress indices for maize. *Agricultural Water Management*, *156*, 51–62.

Dettinger, M. (2005). *Changes in streamflow timing in the western United States in recent decades... from the National Streamflow Information Program*. *Fact Sheet*. https://doi.org/10.3133/fs20053018

Divine, D., Sibray, S. S. (2017). *An Overview of Secondary Aquifers in Nebraska*. *University of Nebraska–Lincoln, Conservation and Survey Division, Educational Circular No. 26*.

English, M. (1990). Deficit irrigation. I: Analytical framework. *Journal of Irrigation and Drainage Engineering*, *116*(3), 399–412.

Erdem, Y., Şehirali, S., Erdem, T., Kenar, D. (2006). Determination of crop water stress index for irrigation scheduling of bean (Phaseolus vulgaris L.). *Turkish Journal of*

Agriculture and Forestry, *30*(3), 195–202.

Fereres, E., Soriano, M. A. (2006). Deficit irrigation for reducing agricultural water use. *Journal of Experimental Botany*, *58*(2), 147–159.

Gardner, B. R., Nielsen, D. C., Shock, C. C. (1992a). Infrared thermometry and the crop water stress index. I. History, theory, and baselines. *Journal of Production Agriculture*, *5*(4), 462–466.

Gardner, B. R., Nielsen, D. C., Shock, C. C. (1992b). Infrared thermometry and the crop water stress index. II. Sampling procedures and interpretation. *Journal of Production Agriculture*, *5*(4), 466–475.

Geerts, S., Raes, D. (2009). Deficit irrigation as an on-farm strategy to maximize crop water productivity in dry areas. *Agricultural Water Management*, *96*(9), 1275–1284.

Gontia, N. K., Tiwari, K. N. (2008). Development of crop water stress index of wheat crop for scheduling irrigation using infrared thermometry. *Agricultural Water Management*, *95*(10), 1144–1152.

Han, M., Zhang, H., DeJonge, K. C., Comas, L. H., Gleason, S. (2018). Comparison of three crop water stress index models with sap flow measurements in maize. *Agricultural Water Management*, *203*(March), 366–375. https://doi.org/10.1016/j.agwat.2018.02.030

Hipps, L. E., Asrar, G., Kanemasu, E. T. (1985). A theoretically-based normalization of environmental effects on foliage temperature. *Agricultural and Forest Meteorology*, *35*(1–4), 113–122.

Idso, S. B. (1982). Non-water-stressed baselines: a key to measuring and interpreting plant water stress. *Agricultural Meteorology*, *27*(1–2), 59–70.

Idso, S. B., Jackson, R. D., Pinter Jr, P. J., Reginato, R. J., Hatfield, J. L. (1981). Normalizing the stress-degree-day parameter for environmental variability. *Agricultural Meteorology*, *24*, 45–55.

Irmak, S. (2014). Interannual variation in long-term center pivot–irrigated maize evapotranspiration and various water productivity response indices. I: Grain yield, actual and basal evapotranspiration, irrigation-yield production functions, evapotranspiration-yield produc. *Journal of Irrigation and Drainage Engineering*, *141*(5), 4014068.

Irmak, S., Haman, D. Z., Bastug, R. (2000). Determination of crop water stress index for irrigation timing and yield estimation of corn. *Agronomy Journal*, *92*(6), 1221–1227.

Irmak, S., Odhiambo, L. O., Kranz, W. L., Eisenhauer, D. E. (2011). Irrigation efficiency and uniformity, and crop water use efficiency.

Irmak, S., Rees, J. M., Zoubek, G. L., van DeWalle, B. S., Rathje, W. R., DeBuhr, R., … Christiansen, A. P. (2010). Nebraska agricultural water management demonstration network (NAWMDN): Integrating research and extension/outreach. *Applied Engineering in Agriculture*, *26*(4), 599–613.

Irmak, S., Rudnick, D. (2014). Corn Irrigation Management Under Water-Limiting Conditions. Retrieved from http://extensionpublications.unl.edu/assets/pdf/ec2007.pdf

Jackson, R. D., Reginato, R. J., Idso, S. B. (1977). Wheat canopy temperature: a practical tool for evaluating water requirements. *Water Resources Research, 13*(3), 651–656.

Jones, H. G. (1999). Use of infrared thermometry for estimation of stomatal conductance as a possible aid to irrigation scheduling. *Agricultural and Forest Meteorology, 95*(3), 139–149.

Kuşçu, H., Turhan, A., Demir, A. O. (2014). The response of processing tomato to deficit irrigation at various phenological stages in a sub-humid environment. *Agricultural Water Management, 133*, 92–103.

LI-COR, E. (2016). *LAI-2200C Plant Canopy Analyzer Instruction Manual*.

Liang, W., Qiao, X., Possignolo, Isabella DeJonge, K., Irmak, S., Heeren, D., Rudnick, D. (2019). Utilizing Digital Image Processing and Two Source Energy Balance Model for the Estimation of Evapotranspiration of Dry Edible Beans in Western Nebraska. *Manuscript Submitted for Publication.*

Mahmoudzadeh Varzi, M., Trout, T. J., DeJonge, K. C., Oad, R. (2019). Optimal water allocation under deficit irrigation in the context of Colorado water law. *Journal of Irrigation and Drainage Engineering, 145*(5), 5019003.

Martin, D. L., Stegman, E. C., Fereres, E. (1990). Irrigation scheduling principles. *IN: Management of Farm Irrigation Systems. American Society of Agricultural Engineers, St. Joseph, MI. 1990. p 155-203, 19 Fig, 9 Tab, 81 Ref.*

Medeiros, G. A., Arruda, F. B., Sakai, E. (2005). Crop coefficient for irrigated beans derived using three reference evaporation methods. *Agricultural and Forest*

Meteorology, *135*(1–4), 135–143.

Medeiros, G. A., Arruda, F. B., Sakai, E., Fujiwara, M. (2001). The influence of crop canopy on evapotranspiration and crop coefficient of beans (Phaseolus vulgaris L.). *Agricultural Water Management*, *49*(3), 211–224.

Meireles, E. J. L., Pereira, A. R., Sentelhas, P. C., Stone, L. F., Zimmermann, F. J. P. (2002). Calibration and test of the cropgro-dry bean model for edaphoclimatic conditions in the savanas of central Brazil. *Scientia Agricola*, *59*(4), 723–729.

Nemeskéri, E., Molnár, K., Vígh, R., Nagy, J., Dobos, A. (2015). Relationships between stomatal behaviour, spectral traits and water use and productivity of green peas (Pisum sativum L.) in dry seasons. *Acta Physiologiae Plantarum*, *37*(2), 34.

Nielsen, D. C. (1990). Scheduling irrigations for soybeans with the Crop Water Stress Index (CWSI). *Field Crops Research*, *23*(2), 103–116. https://doi.org/10.1016/0378-4290(90)90106-L

Nielsen, D. C., Gardner, B. R. (1987). Scheduling Irrigations for Corn with the Crop Water Stress Index (CWSI). *Applied Agricultural Research*, *2*(5), 295–300.

Payero, J. O., Tarkalson, D. D., Irmak, S., Davison, D., Petersen, J. L. (2009). Effect of timing of a deficit-irrigation allocation on corn evapotranspiration, yield, water use efficiency and dry mass. *Agricultural Water Management*, *96*(10), 1387–1397.

Pinter, P., Reginato, R. J. (1982). A Thermal Infrared Technique for Monitoring Cotton Water Stress and Scheduling Irrigations e. *Transactions of the ASAE*, *25*(6), 1651–1655.

Rudnick, D. R., Djaman, K., Irmak, S. (2015). Performance analysis of capacitance and electrical resistance-type soil moisture sensors in a silt loam soil. *Transactions of the ASABE*, *58*(3), 649–665.

Scanlon, B. R., Faunt, C. C., Longuevergne, L., Reedy, R. C., Alley, W. M., McGuire, V. L., McMahon, P. B. (2012). Groundwater depletion and sustainability of irrigation in the US High Plains and Central Valley. *Proceedings of the National Academy of Sciences*, *109*(24), 9320–9325.

Sharkey, T., Seemann, J. (1989). Mild Water Stress Effects on Carbon-Reduction-Cycle Intermediates, Ribulose Bisphosphate Carboxylase Activity, and Spatial Homogeneity of Photosynthesis in Intact Leaves. *Plant Physiology*, *89*, 1060–1065.

Simsek, M., Comlekcioglu, N., Ozturk, I. (2011). The effects of the regulated deficit irrigation on yield and some yield components of common bean (Phaseolus vulgaris L.) under semi-arid conditions. *African Journal of Biotechnology*, *10*(20), 4057–4064.

Taghvaeian, S., Chávez, J., Hansen, N. (2012). Infrared thermometry to estimate crop water stress index and water use of irrigated maize in Northeastern Colorado. *Remote Sensing*, *4*(11), 3619–3637.

Taghvaeian, S., Chávez, J. L., Bausch, W. C., DeJonge, K. C., Trout, T. J. (2014). Minimizing instrumentation requirement for estimating crop water stress index and transpiration of maize. *Irrigation Science*, *32*(1), 53–65.

Tari, A. F. (2016). The effects of different deficit irrigation strategies on yield, quality, and water-use efficiencies of wheat under semi-arid conditions. *Agricultural Water*

Management, *167*, 1–10.

Topp, G. C., Davis, J. L., Annan, A. P. (1980). Electromagnetic determination of soil water content: Measurements in coaxial transmission lines. *Water Resources Research*, *16*(3), 574–582.

Ucar, Y., Kadayifci, A., Yilmaz, H. I., Tuylu, G. I., Yardimci, N. (2009). The effect of deficit irrigation on the grain yield of dry bean (Phaseolus vulgaris L.) in semiarid regions. *Spanish Journal of Agricultural Research*, *7*(2), 474–485.

Urrea, C. A., Cruzado, E. V. (2018). *2018 Nebraska Dry Bean Variety Trials*. Retrieved from https://cropwatch.unl.edu/varietytest/othercrops

Urrea, C. A., Cruzado, E. V. (2019). *2019 Nebraska Dry Bean Variety Trials*. Retrieved from https://cropwatch.unl.edu/varietytest/othercrops

USDA FRIS. (2008). Farm and Ranch Irrigation Survey (2008). *2007 Census of Agriculture*, *3*(Part 1), 216. Retrieved from http://www.agcensus.usda.gov/Publications/2002/FRIS/fris03.pdf

USDA FRIS. (2013). Farm and Ranch Irrigation Survey (2013). *Census of Agriculture*, *3*. Retrieved from http://www.agcensus.usda.gov/Publications/2007/Online_Highlights/Farm_and_Ranch_Irrigation_Survey/index.php

Yazar, A., Howell, T. A., Dusek, D. A., Copeland, K. S. (1999). Evaluation of crop water stress index for LEPA irrigated corn. *Irrigation Science*, *18*(4), 171–180.

Yonts, C. D., Haghverdi, A., Reichert, D. L., Irmak, S. (2018). Deficit irrigation and

surface residue cover effects on dry bean yield, in-season soil water content and irrigation water use efficiency in western Nebraska high plains. *Agricultural Water Management*, *199*, 138–147.

A. Appendix

A.1. Creating precise plot maps to develop prescription irrigation maps

The first task of creating a precise plot map was the collection of boundary points of the field using a GPS. In this study coordinated were recorded using a Trimble GPS (Catalyst, Trimble Navigation Limited, Sunnyvale, California, USA) with a RTK subscription of ± 0.02 m accuracy. Once boundary points were obtained, plots were designed using the tool "Grid Index Features" in ArcGIS Pro (Figure A.1) and the irrigation shapefile was generated. In attribute table, columns were added with details about treatments (Figure A.2).

Once plot maps were designed, irrigation shapefile was added to FieldMAP (Lindsay Corporation, Omaha, NE, USA). Alleys were not included in the irrigation shapefile to account for the transition of linear system when switching from one treatment to another. Once the irrigation shapefile was added to FieldMAP, a similar layout to the one in Figure A.3 appeared on FieldMAP. After selecting option called "Rate table" in FieldMAP, data was entered manually in the rate table. Figure A.4 is a screen shot of an example of rate table. Once rate table was completed, a shapefile layout similar to Figure A.5 was generated by the software. Colors varied depending on irrigation depth each plot was supposed to receive for that irrigation event, where dark blue represented highest irrigation depth and red no irrigation.

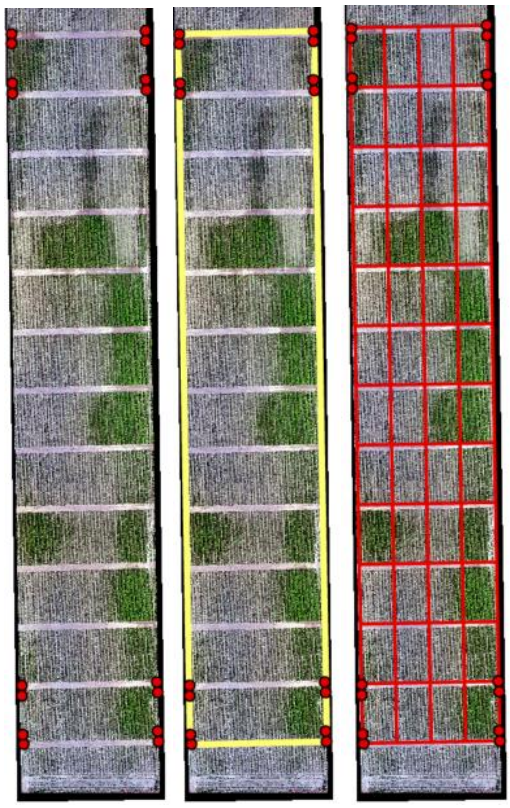

Figure A.1. Steps Used to create plot map using ArcGIS PRO. Left image shows coordinate points collected with Trimble GPS; middle image shows the outside boundary created in ArcGIS; and right image shows the plots generated in ArcGIS using Grid Index Features Tool.

beans_irr_plots_2019_projected

Field: Add Delete Calculate | Selection: Zoom To Switch Clear Delete

OID	Shape	PageName	PageNumbe	Span	Crop	Trt	Combined	Treat_num
6	Polygon	B1	6	R3	Beans	100	R3Beans100	4
7	Polygon	B2	7	R3	Beans	25_75_50	R3Beans25_75_50	7
8	Polygon	B3	8	R3	Beans	0	R3Beans0	1
9	Polygon	B4	9	R3	Beans	50_100_50	R3Beans50_100_50	6
11	Polygon	C1	11	R3	Beans	66	R3Beans66	3
12	Polygon	C2	12	R3	Beans	100_75_50	R3Beans100_75_50	8
13	Polygon	C3	13	R3	Beans	66	R3Beans66	3
14	Polygon	C4	14	R3	Beans	33	R3Beans33	2
16	Polygon	D1	16	R3	Beans	50_100_50	R3Beans50_100_50	6
17	Polygon	D2	17	R3	Beans	0	R3Beans0	1
18	Polygon	D3	18	R3	Beans	100	R3Beans100	4
19	Polygon	D4	19	R3	Beans	100_75_50	R3Beans100_75_50	8
21	Polygon	E1	21	R3	Beans	33	R3Beans33	2
22	Polygon	E2	22	R3	Beans	133	R3Beans133	5

Figure A.2. Attribute table in ArcGIS for irrigation plots.

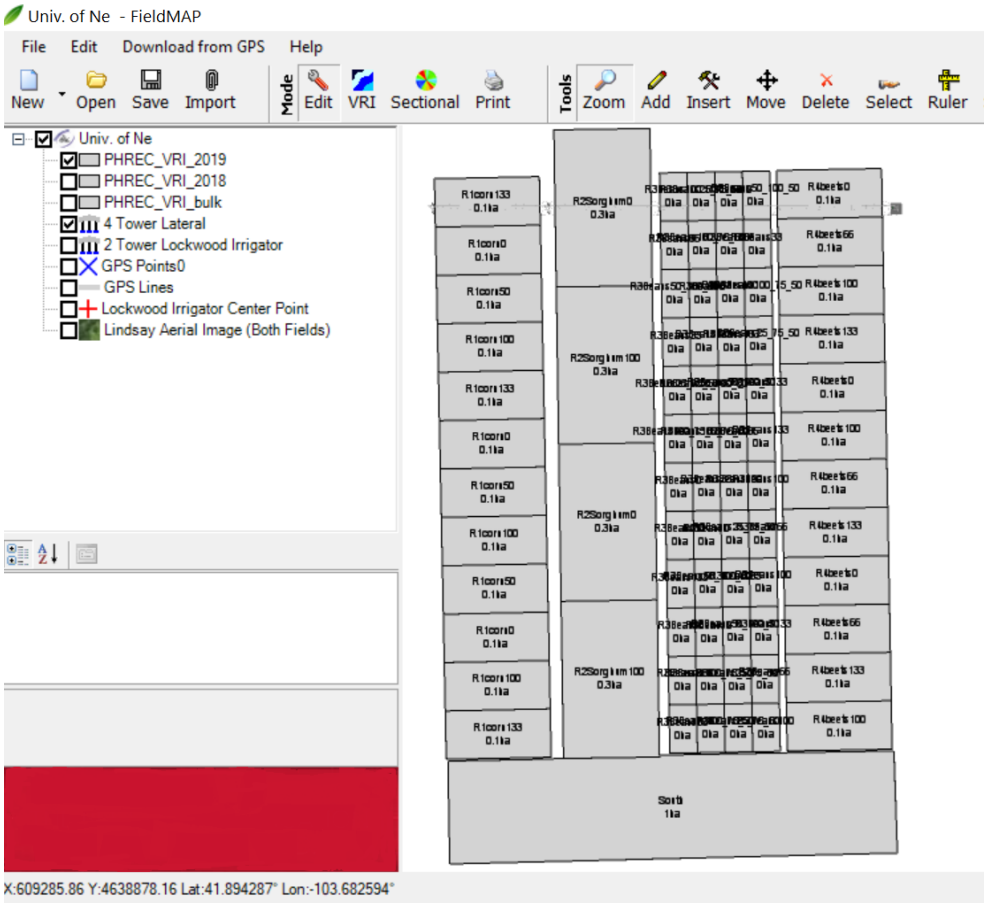

Figure A.3. Screen shots of FieldMAP software showing plot map shapefile.

	Area Name	Current Value	New Value
▶	R1com0 (3)	-10	-10
	R1com100 (3)	0.75	0.75
	R1com133 (3)	1	1
	R1com50 (3)	0.375	0.375
	R2Sorghum0 (2)	-10	-10
	R2Sorghum100 (2)	1	1
	R3Beans0 (6)	-10	-10
	R3Beans100 (6)	0.5	0.5
	R3Beans100_75_50 (6)	-10	-10
	R3Beans133 (6)	0.665	0.665
	R3Beans25_75_50 (6)	0.125	0.125
	R3Beans33 (6)	0.16499999999999998	0.16499999999999998
	R3Beans50_100_50 (6)	0.25	0.25
	R3Beans66 (6)	0.32999999999999996	0.32999999999999996
	R4beets0 (3)	-10	-10
	R4beets100 (3)	0.75	0.75
	R4beets133 (3)	1	1
	R4beets66 (3)	0.49499999999999994	0.49499999999999994
	South	0.15	0.15

Figure A.4. Rate table with irrigation depths for different treatments.

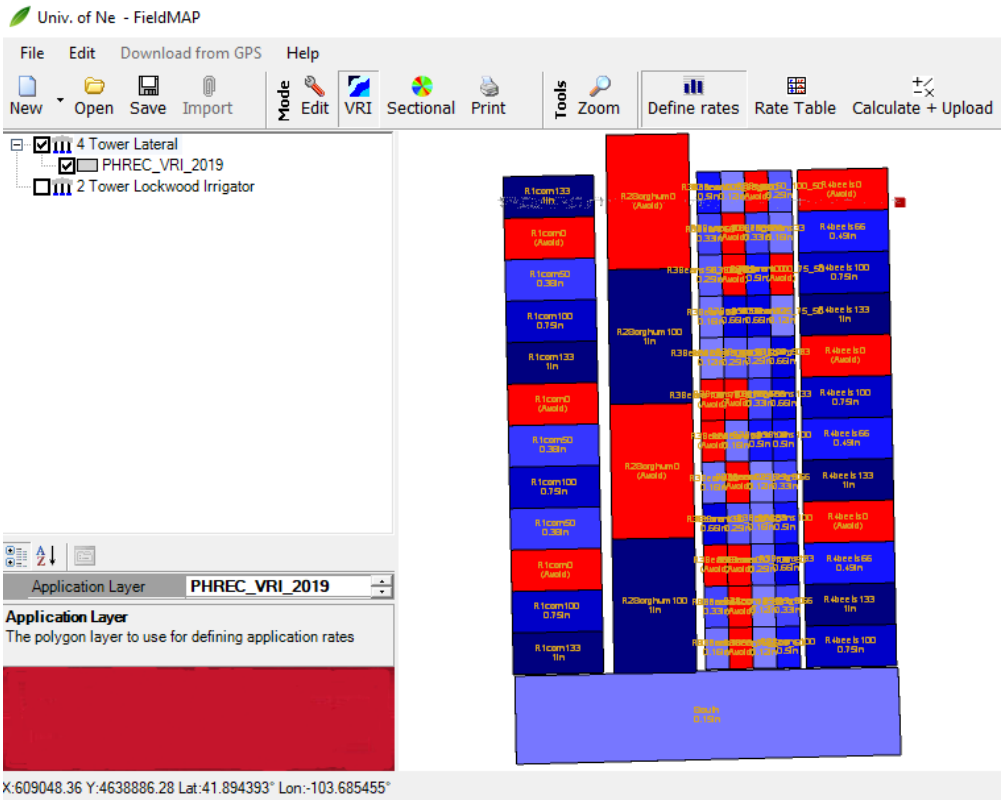

Figure A.5. Screen shots of FielfMAP software showing plot map and different irrigation depths (colors).

Once irrigation plan was finished, the file was saved using option “Save as old folder plan” in FieldMap to a flash drive. The irrigation plan had to be manually uploaded into the Precision VRI panel in the linear irrigation system (located just beside the overall control panel of linear system) (Figure A.6 A). Figure A.6 B shows the Precision VRI box and its USB port at the bottom of panel where files were uploaded. Figure A.7 shows two screenshots that appear in the Precision VRI panel. Figure A.7 A shows the overview screen and Figure A.7 B shows the status of each nozzle, which is used to monitor if nozzles are responding to the wireless control nodes.

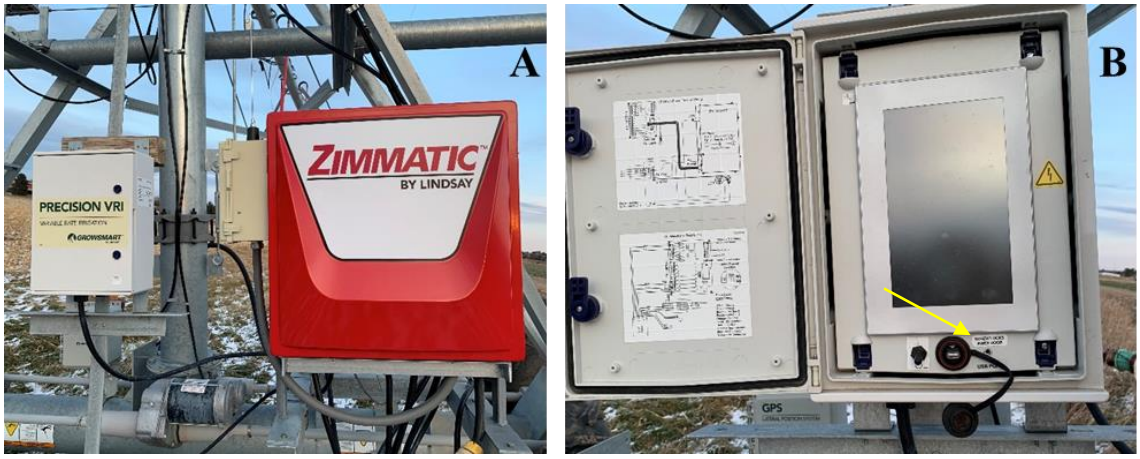

Figure A.6. Precision VRI and linear system control panels (A). Precision VRI box and USB port where irrigation plan is uploaded (yellow arrow) (B).

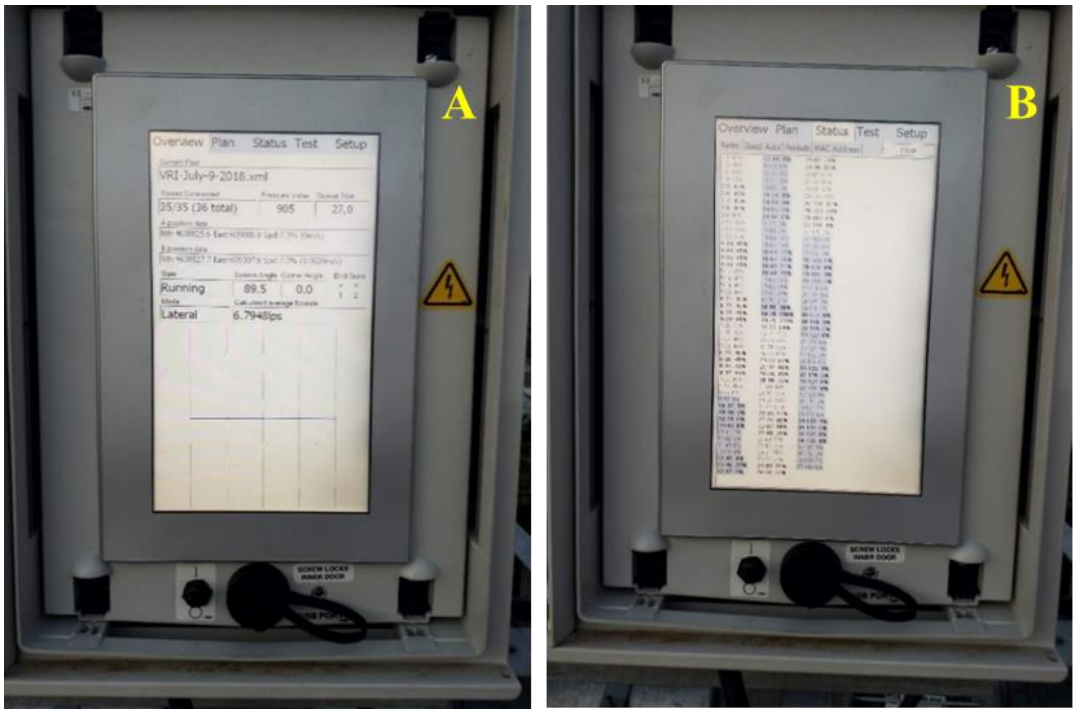

Figure A.7. Screenshots of Precision VRI panel. Overview screen (A). Status screen showing different nozzle groups (not highlighted/highlighted) (B). Each group of nozzle represents a different span of the linear system.

A.2. Codes used in Data Loggers to collect and save data from sensors.

```
'2018 Data logger program
'Program created for campbell CR300 datalogger
'2 IRT sensors

'{
'Declare Variables and Units---------
   '{
   Dim CounterIRT_north
   Dim CounterIRT_south

   Public BattV

   'Rename all the sensors-----------

   Alias ApogeeIRT_north(1) = TargetTC_north
   Alias ApogeeIRT_north(2) = BodyTC_north
   Alias ApogeeIRT_south(1) = TargetTC_south
   Alias ApogeeIRT_south(2) = BodyTC_south

   'Units----------------
   Units BattV=Volts

   Units TargetTC_north=Deg C
   Units BodyTC_north=Deg C
   Units TargetTC_south=Deg C
   Units BodyTC_south=Deg C

   '}

   'Define Data Tables---------------
   '{
   DataTable(average,True,-1)
     DataInterval(0,30,min,0)
     Minimum(1,BattV,FP2,0,1)

     'Apogee IRT and Oxygen
     Average(1,TargetTC_north,IEEE4,False)
     Average(1,BodyTC_north,IEEE4,False)
     Average(1,TargetTC_south,IEEE4,False)
     Average(1,BodyTC_south,IEEE4,False)

   EndTable

'Main Program:--------------------
   '{
   BeginProg

     SW12(1) 'turn on 12v power
     Scan(10,min,0,0)'Main Scan

     Battery(BattV)
```

```
        'Apogee IRT--
        '{
        For CounterIRT_north = 1 To 2
          ApogeeIRT_north(CounterIRT_north) = -1000
        Next
        SDI12Recorder(ApogeeIRT_north(),C1,1,"M!",1,0)

         For CounterIRT_south = 1 To 2
          ApogeeIRT_south(CounterIRT_south) = -1000
        Next
        SDI12Recorder(ApogeeIRT_south(),C1,2,"M!",1,0)

        '}

                CallTable average


     NextScan
   EndProg
   '}
'}
```

```
'2019 Data logger program
'Program created for campbell CR300 datalogger
'2 IRT sensors

'{
'Declare Variables and Units---------
   '{
   Dim CounterIRT_north
   Dim CounterIRT_south
   Public BattV

   'SDI sensors arrays
   Public ApogeeIRT_north(2) 'address 1
   Public ApogeeIRT_south(2) 'address 2


   'Rename all the sensors-----------

   Alias ApogeeIRT_north(1) = TargetTC_north
   Alias ApogeeIRT_north(2) = BodyTC_north
   Alias ApogeeIRT_south(1) = TargetTC_south
   Alias ApogeeIRT_south(2) = BodyTC_south

   'Units----------------
   Units BattV=Volts

   Units TargetTC_north=Deg C
   Units BodyTC_north=Deg C
   Units TargetTC_south=Deg C
   Units BodyTC_south=Deg C
   '}

   'Define Data Tables---------------
   '{
   DataTable(average,True,-1)
     DataInterval(0,5,min,0)
     Minimum(1,BattV,FP2,0,1)

     'Apogee IRT and Oxygen
     Average(1,TargetTC_north,IEEE4,False)
     Average(1,BodyTC_north,IEEE4,False)
     Average(1,TargetTC_south,IEEE4,False)
     Average(1,BodyTC_south,IEEE4,False)

   EndTable


'Main Program:--------------------
   '{
   BeginProg

     SW12(1) 'turn on 12v power
     Scan(1,min,0,0)'Main Scan

       Battery(BattV)
```

```
        'Apogee IRT--
        '{
        For CounterIRT_north = 1 To 2
          ApogeeIRT_north(CounterIRT_north) = -1000
        Next
        SDI12Recorder(ApogeeIRT_north(),C1,1,"M1!",1,0)

         For CounterIRT_south = 1 To 2
          ApogeeIRT_south(CounterIRT_south) = -1000
        Next
        SDI12Recorder(ApogeeIRT_south(),C1,2,"M1!",1,0)
        '}

           CallTable average

    NextScan
  EndProg
  '}
'}
```